

Contextual Stochastic Vehicle Routing with Time Windows

Breno Serrano*

School of Management, Technical University of Munich, Germany, breno.serrano@tum.de

Alexandre M. Florio

Amazon.com, Inc., Bellevue, United States, United States of America, aflorio@gmail.com

Stefan Minner

School of Management and Munich Data Science Institute, Technical University of Munich, Germany,
stefan.minner@tum.de

Maximilian Schiffer

School of Management and Munich Data Science Institute, Technical University of Munich, Germany, schiffer@tum.de

Thibaut Vidal

Département de Mathématiques et de Génie Industriel, Polytechnique Montréal, Canada, thibaut.vidal@polymtl.ca

Abstract. We study the vehicle routing problem with time windows (VRPTW) and stochastic travel times, in which the decision-maker observes related contextual information, represented as feature variables, before making routing decisions. Despite the extensive literature on stochastic VRPs, the integration of feature variables has received limited attention in this context. We introduce the contextual stochastic VRPTW, which minimizes the total transportation cost and expected late arrival penalties conditioned on the observed features. Since the joint distribution of travel times and features is unknown, we present novel data-driven prescriptive models that use historical data to provide an approximate solution to the problem. We distinguish the prescriptive models between point-based approximation, sample average approximation, and penalty-based approximation, each taking a different perspective on dealing with stochastic travel times and features. We develop specialized branch-price-and-cut algorithms to solve these data-driven prescriptive models. In our computational experiments, we compare the out-of-sample cost performance of different methods on instances with up to one hundred customers. Our results show that, surprisingly, a feature-dependent sample average approximation outperforms existing and novel methods in most settings.

Keywords. Stochastic vehicle routing; Data-driven optimization; Machine learning.

* Corresponding author

Declarations of interest: none

1. Introduction

The vehicle routing problem (VRP) is one of the most studied problems in operations research, with the majority of papers focusing on deterministic variants, in which the decision-maker has complete information regarding the model parameters. In practice, VRPs have many sources of uncertainty, e.g., related to travel times, demands, or service times, which stimulated research interest in stochastic optimization models for VRPs. However, many studies on stochastic VRPs consider stylized problems and assume that the uncertain parameters of the optimization problem have known probability distributions.

With the growing availability of data, decision-makers can harness historical data on the uncertain parameters in addition to correlated contextual information, represented as feature variables, to improve uncertainty representation in VRP models. The benefits of contextual optimization for decision-making problems under uncertainty are evident in works from many fields (see, e.g., Sadana et al. 2023). However, within the VRP literature, integrating feature variables related to uncertain parameters has received limited attention. We address this research gap and directly incorporate contextual information into the classical VRP framework.

Specifically, we study the vehicle routing problem with time windows (VRPTW) and uncertain travel times, in which the decision-maker observes related features before making routing decisions. For example, the decision-maker may use contextual information about road closures, seasonal events, or the day of the week to improve routing decisions. To capture the dependence of the optimization problem on external features, we introduce the *contextual stochastic* VRPTW, which minimizes the total transportation cost and expected late arrival penalties conditioned on a set of observed features. We present prescriptive models that use historical data to provide an approximate solution to the problem. We distinguish the data-driven prescriptive models between point-based approximation, sample average approximation (SAA), and penalty-based approximation, each taking a different perspective in dealing with uncertain travel times and features. In particular, point-based approximation models correspond

to the surrogate problem in which travel times are fixed to some estimated values given, e.g., by using a predictive model. In contrast, SAA models capture travel time variability by considering a set of travel time scenarios. In this setting, the decision-maker can take the observed features into account either by associating a feature-dependent weight function to each training observation or by directly constructing feature-dependent travel time scenarios. Finally, we present a penalty-based approximation model, which consists of a predictive model that is trained to directly predict late arrival penalties from features. We develop specialized branch-price-and-cut (BP&C) algorithms and compare the prescriptive models in computational experiments.

1.1. Related Work

We identified two main research streams in the related literature. Specifically, we start with a review of related works on stochastic VRPs and then discuss data-driven stochastic optimization problems that consider the presence of features for different problem settings beyond VRPs.

Stochastic VRPs. Numerous works have investigated stochastic variants of the VRP, e.g., with stochastic demands, travel times, or service times, among other sources of uncertainty. The three most common modeling approaches from the literature are based on robust optimization (RO), chance-constrained programming (CCP), and two-stage stochastic programming with recourse (SPR). Similarly to our paper, many SPR formulations assume a simple recourse policy consisting of a penalty, e.g., for late or early arrivals when time windows are considered. For an introduction to stochastic VRPs, we refer the reader to Gendreau et al. (2014) and Oyola et al. (2017, 2018).

The seminal work of Laporte et al. (1992) introduced an uncapacited VRP with stochastic service and travel times. Kenyon and Morton (2003) extended the work of Laporte et al. (1992) by focusing on minimizing the completion time instead of the total transportation cost. Li et al. (2010) considered time window constraints, extending the formulations of Laporte et al. (1992) to the stochastic VRPTW, for which they proposed a heuristic based on tabu search. Taş et al. (2014b) later solved a VRPTW

under independently gamma-distributed travel times, in which early and late service are permitted but penalized. Their objective minimized the sum of transportation costs and the expected early and late arrival penalties. In contrast to Taş et al. (2014b), we make no assumptions about the distribution of travel times. In addition, we assume that early service is forbidden, which increases the problem difficulty because the distributions of service start times at customers are truncated (cf. Zhang et al. 2019).

From an RO perspective, Lee et al. (2012) and Adulyasak and Jaillet (2016) studied the stochastic VRP with deadlines (VRP-D), a special case of the VRPTW. Further works by Miranda and Conceição (2016) and Errico et al. (2018) adopted a CCP approach for the VRPTW with stochastic travel and service times, respectively. Zhang et al. (2021) addressed the VRPTW with stochastic travel times and proposed a data-driven distributionally robust optimization model.

Focusing on the capacitated vehicle routing problem (CVRP) under demand uncertainty, Gounaris et al. (2013) proposed an RO formulation, and Ghosal and Wiesemann (2020) and Ghosal et al. (2021) proposed distributionally robust chance-constrained optimization models. Recently, Rostami et al. (2021) considered a CVRP in which travel times are stochastic and statistically correlated. Their bi-objective model minimized the total expected travel time and total variance, assuming that the mean and covariance matrix of the travel times are known.

In terms of different optimization criteria, Jaillet et al. (2016) proposed the *requirements violation* (RV) index, which considers both the probability and magnitude of time window violations. They model a traveling salesman problem with time windows (TSPTW) where early service is permitted, and the total RV measure is minimized. Inspired by the RV index, Zhang et al. (2019) proposed the *essential riskiness* index, which enables a multi-commodity flow formulation of the TSPTW where early service is forbidden.

A number of works implicitly considered the impact of external features by modeling time-dependent travel times. For a review on time-dependent routing problems, we refer the reader to Gendreau et al.

(2015). Dabia et al. (2013) proposed an arc-based formulation for the VRPTW under deterministic time-dependent travel times and Taş et al. (2014a) proposed metaheuristics for the VRPTW with time-dependent and stochastic gamma-distributed travel times. In contrast to time-dependent VRPs, we assume that travel times are time-independent within a service period, and we explicitly model the dependence of travel times on a set of external features.

Despite the extensive literature on stochastic VRPs, previous works considered the presence of contextual information only implicitly, e.g., with time-dependent travel times. Incorporating contextual information into the model can significantly reduce routing costs. Accordingly, we contribute to the current state of the art by proposing novel models and algorithms for the contextual stochastic VRPTW. In addition, we show how to adapt state-of-the-art BP&C techniques when contextual information is available.

Contextual stochastic optimization. Many recent works have investigated the use of contextual information to improve decisions under uncertainty, with applications to transportation, inventory, and operations management, among others. The recent survey by Sadana et al. (2023) reviewed papers on contextual optimization with a focus on models and methods, while the review paper by Mišić and Perakis (2020) discussed recent applications in the operations management literature.

Bertsimas and Kallus (2019) proposed a framework for contextual optimization based on weighted SAA and derived weight functions based on machine learning methods, such as k -nearest neighbors regression, local linear regression, and tree-based methods. The authors applied the framework to a two-stage shipment planning problem and to a multi-product inventory problem. Nearly simultaneously, Bertsimas and McCord (2018) adapted the framework for problems with decision-dependent uncertainties. Bertsimas and McCord (2019) and Bertsimas et al. (2023) extended the framework of Bertsimas and Kallus (2019) to multi-stage and multi-period stochastic optimization problems, respectively. Van Parys and Bennouna (2022) proposed robust formulations based on regularized SAA for

conditional two-stage optimization problems.

Elmachtoub and Grigas (2021) proposed a framework tailored to optimization problems consisting of a linear objective with uncertain coefficients. They used feature data to learn a prediction model for the objective coefficients and adopted a modified loss function that directly leverages the structure of the optimization problem instead of minimizing a standard prediction error, such as the least squares loss. Mandi et al. (2020) extended this framework to solve some discrete combinatorial problems and illustrated their algorithmic improvements on a weighted knapsack problem and a scheduling problem.

In the context of inventory optimization, Beutel and Minner (2012) and Ban and Rudin (2019) studied the data-driven newsvendor problem and proposed models for learning a decision function that predicts order quantities directly from feature observations. Serrano et al. (2024) extended their framework, introducing an integrated approach based on bilevel programming that performs feature selection. Mandl and Minner (2023) studied a multi-period commodity procurement problem under price uncertainty with forward and spot purchase options. They proposed a data-driven model to derive optimal purchase policies based on features, such as economic indicators.

In the context of last-mile delivery operations, Liu et al. (2021) assigned orders to drivers under uncertain service times and considered that drivers' routes may deviate from planned routes. The authors used features, e.g., based on the customers' locations, to learn a prediction model for the drivers' travel times, which is then integrated into the order assignment optimization.

Motivated by the problem of forecasting electricity demands given a set of features, Rios et al. (2015) proposed a scenario generation method based on estimating the distribution of forecast errors, i.e., residuals. Ban et al. (2019) investigated a similar methodology for a multi-stage stochastic procurement problem under uncertain demand, where they learned a regression model that relates features to demands and used the residuals to generate demand samples for a new product. They subsequently solved an SAA model to determine the optimal procurement policy.

Many works in the contextual optimization literature deal with optimization problems that can be

efficiently solved, e.g., that can be modeled as linear programs. In contrast, the VRPTW is a challenging optimization problem, for which many researchers have proposed problem-tailored solution techniques over the last decades. On the one hand, we show how existing contextual optimization methods can be applied to this challenging application. On the other hand, we investigate novel methods that can be generally applied to other contextual optimization problems.

1.2. Contributions

Our work contributes to the research streams outlined in the previous section. First, we introduce a novel formulation for the contextual stochastic VRPTW, in which realizations of travel times are conditioned on a set of related features. Second, we show how existing contextual optimization methods can be applied to the contextual stochastic VRPTW and propose novel data-driven methods leveraging historical data. In particular, we propose a conditional sample average approximation (CSAA) method, a general technique based on SAA for solving contextual optimization problems. Third, we propose a problem-tailored penalty-based prescriptive method that uses machine learning to predict late arrival penalties at customers instead of relying on travel time estimates. Fourth, we describe a specialized BP&C algorithm that is generally applicable to stochastic VRP variants in which the travel times can capture the problem uncertainty, e.g., when uncertain service times or costs can be modeled in terms of uncertain travel times. One key component of our BP&C implementation is the use of completion bounds instead of common dominance rules for discarding labels in the pricing algorithm. Fifth, we conduct computational experiments to compare the proposed prescriptive models and conclude that SAA methods equipped with feature-dependent scenarios show the best average performance, providing solutions that are closest to the full-information benchmark.

The remainder of this paper is organized as follows. Section 2 formally introduces the contextual stochastic VRPTW. Section 3 presents our data-driven prescriptive models. Section 4 describes the corresponding solution methods based on BP&C. Section 5 presents our experimental design and Section 6

discusses computational results. Finally, Section 7 concludes the paper.

2. The Contextual Stochastic VRPTW

We define the contextual stochastic VRPTW on a complete digraph $\mathcal{G} = (\mathcal{V}, \mathcal{A})$, where $\mathcal{V} = \{0, \dots, N\}$ is the set of nodes and $\mathcal{A} = \{(i, j) : i, j \in \mathcal{V}\}$ is the set of arcs. Set $\mathcal{V} \setminus \{0\}$ represents customers, and node 0 denotes the depot. A homogeneous fleet of K vehicles, each with a capacity of Q , is stationed at the depot. Each node $i \in \mathcal{V}$ has known demand q_i and a time window $[e_i, \ell_i]$, $0 \leq e_i \leq \ell_i$. Each arc $(i, j) \in \mathcal{A}$ has a deterministic cost c_{ij} and an uncertain travel time \tilde{t}_{ij} . Throughout the paper, we use a tilde to indicate random variables and follow standard boldfaced notation for vectors and vector-valued functions.

We focus on a setting in which the joint distribution of travel times $\tilde{\mathbf{t}} = [\tilde{t}_{ij}]_{(i,j) \in \mathcal{A}}$ is unknown. The decision-maker observes a set of features, represented by a p -dimensional vector $\mathbf{x} = [x_1, \dots, x_p]$, before the travel times are revealed. Features are exogenous variables that may be travel time predictors, e.g., day of the week, season, events, meteorological data, and road works or closures.

A route is a non-empty sequence of customers $\theta = (v_1, \dots, v_L)$ such that $\sum_{i \in \theta} q_i \leq Q$ and $v_i \neq v_j$ if $i \neq j$. We further define:

$$C_\theta = c_{0v_1} + \sum_{k=2}^L c_{v_{k-1}v_k} + c_{v_L 0} \quad (1)$$

as the transportation cost of route θ . We assume that transportation costs are deterministic and independent of travel times and features, e.g., if drivers have fixed salaries, and if fuel consumption costs can be well approximated considering only the distance traveled. Note that this assumption is not restrictive since all proposed methods can be adapted to a setting with uncertain costs by using (simplified variants of) the methodology presented in this work.

All routes start at the depot. We assume that service times equal to 0, without loss of generality, as a positive service time at a customer can be added to the travel times of its outgoing arcs. Early service is forbidden, such that in case of early arrival at customer i , the vehicle must wait until e_i before

service can start. Given a route $\theta = (v_1, \dots, v_L)$ and realized travel times $\mathbf{t} = [t_{ij}]_{(i,j) \in \mathcal{A}}$, we define the *arrival time* $a_\theta(v_k; \mathbf{t})$ at customer $v_k \in \theta$ as:

$$a_\theta(v_k; \mathbf{t}) = \begin{cases} t_{0v_1}, & \text{if } k = 1, \\ \max\{e_{v_{k-1}}, a_\theta(v_{k-1}; \mathbf{t})\} + t_{v_{k-1}v_k}, & \text{if } k \in \{2, \dots, L\}. \end{cases} \quad (2)$$

Since early arrivals are not permitted, the instant when customer $v_k \in \theta$ is served, i.e., the *service start time* at customer v_k , is given by:

$$s_\theta(v_k; \mathbf{t}) = \max\{e_{v_k}, a_\theta(v_k; \mathbf{t})\}. \quad (3)$$

Equivalently, $s_\theta(v_k; \mathbf{t}) + t_{v_k v_{k+1}} = a_\theta(v_{k+1}; \mathbf{t})$. Moreover, a penalty of $\pi(a_\theta(v_k; \mathbf{t}) - \ell_{v_k})$ occurs in case of late arrivals at customer v_k , where $\pi(\cdot)$ is a nondecreasing penalty function such that $\pi(0) = 0$. For notational convenience, we define $\pi(u) = 0$ if $u < 0$.

With Θ being the set of all routes, we represent a solution to the contextual stochastic VRPTW by a vector $\mathbf{z} = [z_\theta]_{\theta \in \Theta} \in \{0, 1\}^{|\Theta|}$, where $z_\theta = 1$ if and only if route θ belongs to the solution. Accordingly, the feasible region is determined by the set:

$$\mathcal{Z}_\Theta = \left\{ \mathbf{z} \in \{0, 1\}^{|\Theta|} \left| \begin{array}{l} \sum_{\theta \in \Theta} \mathbb{1}(i \in \theta) z_\theta = 1, \quad i \in \mathcal{V} \setminus \{0\}, \quad (\text{a}) \\ \sum_{\theta \in \Theta} z_\theta \leq K \quad (\text{b}) \end{array} \right. \right\}, \quad (4)$$

where $\mathbb{1}(\cdot)$ is the indicator function. The partitioning constraints (4a) ensure that all customers are visited once, and constraint (4b) enforces that no more than K vehicles are used.

We formulate the contextual stochastic VRPTW as a two-stage stochastic program:

$$\mathbf{z}^*(\mathbf{x}) = \arg \min_{\mathbf{z} \in \mathcal{Z}_\Theta} C(\mathbf{z}) + \mathbb{E} [Q(\mathbf{z}, \tilde{\mathbf{t}}) \mid \tilde{\mathbf{x}} = \mathbf{x}], \quad (\text{CS-VRPTW})$$

where the first-stage objective corresponds to the total transportation costs $C(\mathbf{z}) = \sum_{\theta \in \Theta} C_\theta z_\theta$, and the second-stage recourse policy consists of penalizing late arrivals, leading to the second-stage value function:

$$Q(\mathbf{z}, \mathbf{t}) = \sum_{\theta \in \Theta} \left(\sum_{i \in \theta} \pi(a_\theta(i; \mathbf{t}) - \ell_i) \right) z_\theta. \quad (5)$$

We further denote by $f_{\Theta}(\mathbf{z}, \mathbf{t})$ the value of a solution \mathbf{z} under realized travel times \mathbf{t} :

$$f_{\Theta}(\mathbf{z}, \mathbf{t}) = C(\mathbf{z}) + Q(\mathbf{z}, \mathbf{t}). \quad (6)$$

Thus, we can equivalently express the CS-VRPTW as:

$$\mathbf{z}^*(\mathbf{x}) = \arg \min_{\mathbf{z} \in \mathcal{Z}_{\Theta}} \mathbb{E} [f_{\Theta}(\mathbf{z}, \tilde{\mathbf{t}}) \mid \tilde{\mathbf{x}} = \mathbf{x}]. \quad (7)$$

Since the joint distribution of travel times and features is unknown, we approximate the conditional expectation in the CS-VRPTW formulation using data-driven prescriptive models that leverage historical travel times and features.

3. Data-driven Prescriptive Models

As the contextual stochastic VRPTW formulation cannot be solved directly, we discuss approximate and computationally tractable reformulations in the following. We assume that the decision-maker has access to historical travel times for the last n periods, represented by the $n \times |\mathcal{A}|$ matrix $\mathbf{T} = [\mathbf{t}^1, \dots, \mathbf{t}^n]^{\top}$, where $\mathbf{t}^k = [t_{ij}^k]_{(i,j) \in \mathcal{A}}$ are the travel times observed at period k . Further, the decision-maker has access to feature data for the last n periods, represented by the $n \times p$ matrix $\mathbf{X} = [\mathbf{x}^1, \dots, \mathbf{x}^n]^{\top}$, where $\mathbf{x}^k = [x_1^k, \dots, x_p^k]$ contains the realizations of p features at period k . We assume w.l.o.g. that $x_1^k = 1$ for all $k \in \{1, \dots, n\}$. We further assume that the data is low-dimensional, i.e., $p < n$, and that \mathbf{X} has full rank. The decision-maker solves the CS-VRPTW for period $n + 1$, having observed the feature vector \mathbf{x}^{n+1} but without knowing the realization of travel times.

3.1. Point-based Approximation

We simplify the CS-VRPTW by fixing the travel times to point estimates $\hat{\mathbf{t}} = [\hat{t}_{ij}]_{(i,j) \in \mathcal{A}}$ and considering the deterministic optimization problem:

$$\hat{\mathbf{z}}_{\text{D}}^*(\mathbf{x}) = \arg \min_{\mathbf{z} \in \mathcal{Z}_{\Theta}} f_{\Theta}(\mathbf{z}, \hat{\mathbf{t}}) = \arg \min_{\mathbf{z} \in \mathcal{Z}_{\Theta}} C(\mathbf{z}) + Q(\mathbf{z}, \hat{\mathbf{t}}). \quad (\text{P})$$

In this setting, different options to compute $\hat{\mathbf{t}}$ from historical travel times \mathbf{T} and feature data \mathbf{X}

exist. If \mathbf{X} is a poor predictor of \mathbf{T} , then a reasonable option is to set \hat{t}_{ij} to a statistic of $\{t_{ij}^k\}_{k \in \{1, \dots, n\}}$, e.g., the mean, median, or a higher percentile in case more protection against late arrivals is desired. Otherwise, if \mathbf{X} is a good predictor of \mathbf{T} , we may fix travel times to:

$$\hat{\mathbf{t}} = \mathbf{g}(\mathbf{x}^{n+1}; \boldsymbol{\varphi}), \quad (8)$$

where $\mathbf{g} : \mathbb{R}^p \mapsto \mathbb{R}^{|\mathcal{A}|}$ is a travel time prediction model, e.g., a multivariate regression model or a neural network, with parameters $\boldsymbol{\varphi}$ trained from historical travel times and features. The latter approach corresponds to the *predict-then-optimize* (PTO) paradigm (Elmachtoub and Grigas 2021). Since point estimates are used, Model (P) does not capture the impact of travel time variability on the decision cost and thus may yield poor decisions because the effects of under- and over-predicting travel times are not symmetric.

Note that a special case of Model (P) arises when the penalty function is such that $\pi(s) = \infty$ if $s > 0$. In this case, the model reduces to the classical VRPTW with hard time windows, for which efficient exact algorithms exist (cf. Pessoa et al. 2020). For general non-decreasing penalty functions, we solve Model (P) with a tailored BP&C algorithm as described in Section 4.

3.2. Sample Average Approximation

Travel time variability plays a key role in the CS-VRPTW since late arrival penalties grow with the amount of delay. We represent travel time variability in the stochastic model with a set of scenarios $\{\mathbf{t}^\omega\}_{\omega \in \Omega}$, where $\mathbf{t}^\omega = [t_{ij}^\omega]_{(i,j) \in \mathcal{A}}$ is a possible realization of travel times at period $n + 1$, corresponding to scenario $\omega \in \Omega$. We further associate a feature-dependent weight function $\alpha^\omega(\mathbf{x}) : \mathbb{R}^p \mapsto \mathbb{R}$ to each scenario $\omega \in \Omega$ and approximate the conditional expected penalty using weighted SAA:

$$\hat{\mathbf{z}}_s^*(\mathbf{x}) = \arg \min_{\mathbf{z} \in \mathcal{Z}_\Theta} \sum_{\omega \in \Omega} \alpha^\omega f_\Theta(\mathbf{z}, \mathbf{t}^\omega) = \arg \min_{\mathbf{z} \in \mathcal{Z}_\Theta} C(\mathbf{z}) + \sum_{\omega \in \Omega} \alpha^\omega Q(\mathbf{z}, \mathbf{t}^\omega), \quad (S)$$

where we assume, w.l.o.g., that $\sum_{\omega \in \Omega} \alpha^\omega = 1$. Model (S) computes the second-stage cost by SAA (Shapiro et al. 2014). Note that Model (P) is a special case of Model (S) with $|\Omega| = 1$.

Before solving Model (S), the decision-maker must define the set of scenarios Ω . If the feature data

\mathbf{X} are poor predictors of the travel times \mathbf{T} , then a sensible option is to define the travel time scenarios as the historical travel times $\{\mathbf{t}^\omega\}_{\omega \in \Omega} = \{\mathbf{t}^k\}_{k \in \{1, \dots, n\}}$, with $\alpha^\omega = 1/n$ for $\omega \in \Omega$.

3.3. Conditional SAA

To generate feature-dependent scenarios, we specify a probabilistic model for travel times and features. Let $\tilde{\mathbf{x}} = [\tilde{x}_1, \dots, \tilde{x}_p]$ be a random vector representing features before they are revealed at the current period $n + 1$. Then, we assume that travel times (conditioned on $\tilde{\mathbf{x}}$) are given by:

$$\tilde{\mathbf{t}} \mid \tilde{\mathbf{x}} = \mathbf{B}^\top \tilde{\mathbf{x}} + \tilde{\boldsymbol{\varepsilon}}, \quad (9)$$

where \mathbf{B} is a $p \times |\mathcal{A}|$ matrix of constant parameters and $\tilde{\boldsymbol{\varepsilon}} = [\tilde{\varepsilon}_{ij}]_{(i,j) \in \mathcal{A}}$ is a random noise vector following a multivariate distribution with zero mean and unknown covariance matrix $\boldsymbol{\Sigma}$.

The conditional travel times model from Equation (9) generalizes the correlated travel times model by Jaillet et al. (2016) in that $\tilde{x}_1, \dots, \tilde{x}_p$ are not assumed to be independent and the noise terms $\tilde{\varepsilon}_{ij}$ allow for a stronger or weaker dependence between \tilde{t}_{ij} and $\tilde{\mathbf{x}}$ for each arc. Therefore, the feature space may include interaction terms between travel time covariates, which may improve travel time prediction accuracy as non-linearities can be captured. Moreover, the error terms $\tilde{\varepsilon}_{ij}$ may be correlated, so the model allows for correlated travel time variability caused by unanticipated events, e.g., emergency work or traffic incidents.

From historical travel times \mathbf{T} and feature data \mathbf{X} , we estimate matrix \mathbf{B} by least squares:

$$\hat{\mathbf{B}} = (\mathbf{X}^\top \mathbf{X})^{-1} \mathbf{X}^\top \mathbf{T}. \quad (10)$$

Following multivariate analysis theory (Rencher and Christensen 2012), an estimate of the covariance matrix $\boldsymbol{\Sigma}$ is given by:

$$\hat{\boldsymbol{\Sigma}} = \frac{\mathbf{T}^\top \mathbf{T} - \hat{\mathbf{B}}^\top \mathbf{X}^\top \mathbf{T}}{n - p}. \quad (11)$$

Accordingly, if the feature data are good travel time predictors, we obtain a feature-dependent representation of travel time uncertainty at period $n + 1$ by sampling travel times from a multivariate

distribution with mean and covariance given by $\hat{\mathbf{B}}^\top \mathbf{x}^{n+1}$ and $\hat{\mathbf{\Sigma}}$, respectively.

3.4. Residual-based SAA

The conditional SAA model from Section 3.3 requires the decision-maker to make distributional assumptions on travel times to generate feature-dependent scenarios. We present a distribution-free residual-based sample average approximation (RSAA) model based on the residual tree method of Ban et al. (2019). Consider a travel time prediction model $\mathbf{g}(\cdot)$ as introduced in Equation (8) with parameters learned from historical travel times \mathbf{T} and features \mathbf{X} . We compute the prediction error, which we denote as the *residual*, associated with training observation k as:

$$\epsilon^k = \mathbf{g}(\mathbf{x}^k) - \mathbf{t}^k. \quad (12)$$

Given a feature vector \mathbf{x}^{n+1} at period $n+1$, we generate a set of feature-dependent scenarios where scenario k is given by the sum of the model prediction for the observed feature vector and the residual associated with training observation k :

$$\Omega = \left\{ \mathbf{g}(\mathbf{x}^{n+1}; \varphi) + \epsilon^k \right\}_{k=1, \dots, n}. \quad (13)$$

We then solve Model (S) with uniformly weighted residual-based scenarios Ω .

3.5. Late Arrival Penalty Approximation

Instead of leveraging feature data to estimate the travel times distribution, and then using such estimates to approximate the expected penalty of a solution, we can use data to predict penalties directly. We define the penalty-based approximation model:

$$\hat{\mathbf{z}}_p^*(\mathbf{x}) = \arg \min_{\mathbf{z} \in \mathcal{Z}_\Theta} \hat{f}_\Theta(\mathbf{z}, \mathbf{x}) = \arg \min_{\mathbf{z} \in \mathcal{Z}_\Theta} C(\mathbf{z}) + \hat{Q}(\mathbf{z}, \mathbf{x}), \quad (\text{L})$$

where $\hat{Q}(\mathbf{z}, \mathbf{x})$ approximates the conditional expected penalty $\mathbb{E} [Q(\mathbf{z}, \tilde{\mathbf{t}}) \mid \tilde{\mathbf{x}} = \mathbf{x}]$.

By definition, the conditional expected penalty of a solution \mathbf{z} in Equation (5) can be decomposed into the sum of the late arrival penalties at the customers along the routes in \mathbf{z} . Clearly, the predicted penalty at a given customer i along a given route $\theta \in \Theta$ depends on customer and route

characteristics, e.g., the expected penalty is correlated with the position of i in the route or the customer time window, in addition to the features \mathbf{x} related to the travel times. Therefore, we define a feature projection function (FPF), $\mathbf{f} : \mathbb{R}^p \times \Theta \times \mathcal{V} \setminus \{0\} \mapsto \mathbb{R}^{\bar{p}}$, that combines travel time covariates with node and route characteristics to obtain a vector of penalty predictors $\mathbf{y} \in \mathbb{R}^{\bar{p}}$:

$$\mathbf{y} = \mathbf{f}(\mathbf{x}, \theta, i). \quad (14)$$

Essentially, $\mathbf{f}(\mathbf{x}, \theta, i)$ projects \mathbf{x} onto a \bar{p} -dimensional feature space with potential predictors of the penalty at customer $i \in \theta$. We describe the projected features in detail in Appendix A.

A prediction model $h(\cdot)$ outputs late arrival penalty predictions based on the projected features \mathbf{y} given by the FPF. We approximate the expected value \hat{Q} of the second-stage penalty as:

$$\hat{Q}(\mathbf{z}, \mathbf{x}) = \sum_{\theta \in \Theta} \sum_{i \in \theta} h(\mathbf{y}; \mathbf{H}) z_{\theta} \quad (15)$$

where \mathbf{H} denotes the trained parameters of the prediction model $h(\cdot)$.

We adopt a supervised learning setting and build a training dataset with \bar{n} observations of the projected features \mathbf{y}^k and penalties π^k , for $k \in \{1, \dots, \bar{n}\}$. Specifically, we generate the projected features, represented by $\mathbf{Y} = [\mathbf{y}^1, \dots, \mathbf{y}^{\bar{n}}]$, from the original feature data \mathbf{X} , historical travel times \mathbf{T} , and a set of routes Θ . In our experiments, we construct a set Θ of routes by solving the other prescriptive models, i.e., point-based and SAA models, using the BP&C algorithm described in Section 4, and record all routes evaluated during the solution process. The corresponding penalties, represented by $\boldsymbol{\pi} = [\pi^1, \dots, \pi^{\bar{n}}]$, can be computed by propagating the arrival times at each node along the route based on the respective travel times. The learning problem then corresponds to finding the model parameters that minimize some empirical risk of the form:

$$\hat{\mathbf{H}} = \arg \min_{\mathbf{H}} \sum_{k=1}^{\bar{n}} \mathcal{L}(h(\mathbf{y}^k; \mathbf{H}), \pi^k) \quad (16)$$

where \mathcal{L} defines a loss function, e.g., a squared error, and the prediction model can be any supervised regression model, e.g., based on linear regression or neural networks.

4. Solution Methods for the Data-driven Prescriptive Models

We adopt a set-partitioning formulation, where the set of decision variables representing the feasible routes Θ can be exponentially large. To solve the proposed models, we rely on branch-and-price, which is an effective method for solving integer linear programs with a very large number of variables (Barnhart et al. 1998). In vehicle routing, the technique is applied to solve many problem variants that admit a set-partitioning formulation (Costa et al. 2019). We start by introducing the solution method for solving Model (S) in Sections 4.1 and 4.2 before we explain how to adapt the method to solve Model (L) in Section 4.3.

4.1. Column Generation

In branch-and-price, we solve the continuous relaxation of the set-partitioning formulation by column generation. We define a restricted master problem (RMP) considering only a subset $\Theta' \subset \Theta$ of the set of feasible routes, which yields the following linear program:

$$\begin{aligned}
 \min \quad & \sum_{\omega \in \Omega} \alpha^\omega f_{\Theta'}(\mathbf{z}, \mathbf{t}^\omega) & \text{(RMP)} \\
 \text{s.t.} \quad & \sum_{\theta \in \Theta'} \mathbb{1}(i \in \theta) z_\theta = 1, & i \in \mathcal{V} \setminus \{0\} \\
 & \sum_{\theta \in \Theta'} z_\theta \leq K \\
 & 0 \leq z_\theta \leq 1, & \theta \in \Theta'.
 \end{aligned}$$

The column generation procedure repeatedly solves (RMP), identifies routes that correspond to negative reduced cost variables, and adds those routes to Θ' . To this end, we solve the corresponding pricing problem:

$$\min_{\theta \in \Theta} \bar{C}_\theta \triangleq C_\theta + \sum_{\omega \in \Omega} \alpha^\omega \sum_{i \in \theta} \pi(a_\theta(i; \mathbf{t}^\omega) - \ell_i) - \sum_{i \in \theta} \gamma_i - \mu, \quad \text{(PP-S)}$$

where, given a solution to (RMP), $\gamma = [\gamma_i]_{i \in \mathcal{V} \setminus \{0\}}$ and μ are the dual values associated with Constraints (4a) and (4b), respectively. The pricing problem is an elementary shortest path problem with

resource constraints (ESPPRC), which is \mathcal{NP} -hard.

4.2. Pricing Algorithm

We use an extend-and-bound labeling algorithm, where a label represents a partial path from the depot to a customer. The labeling procedure creates new labels by extending partial paths to all feasible customers. For each new label extension, we compute a lower bound on the reduced cost of all routes that can be generated from the label extension, i.e., a completion bound. Then, we discard the label extension if this bound is non-negative.

A label L_θ representing a path θ is a tuple $L_\theta = (i, \bar{C}_\theta, q_\theta, \tau_\theta)$, where $i \in \mathcal{V} \setminus \{0\}$ is the last customer in θ , \bar{C}_θ is the reduced cost, $q_\theta = \sum_{v \in \theta} q_v$ is the cumulated load along θ , and τ_θ is the earliest time at which service can start at customer i if θ is used to reach i :

$$\tau_\theta = \min_{\omega \in \Omega} \{s_\theta(i; \mathbf{t}^\omega)\}, \quad (17)$$

considering all scenarios $\omega \in \Omega$.

If we extend label L_θ along an arc (i, j) , we generate a new path $\theta' = \theta \oplus (i, j)$ with a corresponding label $L_{\theta'} = (j, \bar{C}_{\theta'}, q_{\theta'}, \tau_{\theta'})$, such that:

$$\bar{C}_{\theta'} = \bar{C}_\theta - c_{i0} + c_{ij} + c_{j0} + \sum_{\omega \in \Omega} \alpha^\omega \cdot \pi(a_{\theta'}(j; \mathbf{t}^\omega) - \ell_j) - \gamma_j \quad (18)$$

$$\tau_{\theta'} = \min_{\omega \in \Omega} \{s_{\theta'}(j; \mathbf{t}^\omega)\}. \quad (19)$$

Path θ' is feasible if $q_{\theta'} \leq Q$. Otherwise, it is infeasible, and we discard the new label.

A completion bound $\hat{T}(i, q)$ is a lower bound on the value of the best path starting at customer i and ending at the depot with a total load less than or equal to q . If the following condition holds, then we can discard label L_θ without losing any negative reduced cost route:

$$\bar{C}_\theta + \hat{T}(i, Q - q_\theta) \geq 0. \quad (20)$$

Since we solve the pricing problem multiple times during the execution of the BP&C method, it is important to generate completion bounds quickly. Hence, we employ heuristic algorithms based on a

resource-constrained shortest path (RCSP) problem and based on a knapsack formulation (cf. Florio et al. 2020). Unlike many labeling algorithms from the literature, we do not discard labels based on dominance rules. In order to use dominance rules in our setting, we would need labels to store a resource corresponding to the service start time under each travel time scenario. We leave the investigation of dominance rules and the assessment of their effectiveness for future research.

Resource-Constrained Shortest Path (RCSP) Bound. We derive RCSP bounds by relaxing the elementary requirement of the ESPPRC and enforcing 2-cycle elimination, i.e., we allow paths with cycles only if cycles have a length of at least three customers. Resource constraints correspond to the capacity constraints on the vehicles. We compute a lower bound on the late arrival penalties along a path θ based on the earliest service start time τ_θ . We provide a dynamic programming (DP) algorithm for computing the RCSP bounds in Appendix B, where we apply a time discretization with a time step Δt such that we can efficiently store the optimal value of each subproblem. The DP algorithm solves the following recursive formulation:

$$\widehat{T}_{\text{RCSP}}(i, Q - q_\theta) = -c_{i0} + \min_{\substack{j \in \mathcal{V} \setminus \{0\}: \theta' = \theta \oplus (i, j), \\ j \neq i, \rho(i) \neq j, \\ q_\theta + q_j \leq Q}} \left\{ c_{ij} + \pi(\delta_{\theta'} - \ell_j) - \gamma_j + c_{j0} + \widehat{T}_{\text{RCSP}}(j, Q - q_{\theta'}) \right\}, \quad (21)$$

where $\theta' = \theta \oplus (i, j)$ denotes the extension of path θ along the arc (i, j) and δ_θ is a multiple of Δt representing a lower bound on the service start time of customer $i \in \theta$, such that $\tau_\theta \in [\delta_\theta, \delta_\theta + \Delta t]$. The resulting completion bound expresses the maximum reduced cost decrease from node i given that departure from node i is not before δ_θ .

Proposition 1 *Let θ be a route starting at the depot and ending at customer i with reduced cost \overline{C}_θ and cumulative demand q_θ . Let $L_{\theta'}$ be a label extension associated with the route $\theta' = \theta \oplus \mathcal{E}$, where $\mathcal{E} = (u_1, u_2, \dots, u_L)$ is a path such that $u_j \notin \theta, \forall u_j \in \mathcal{E}$, and $q_{\theta'} \leq Q$. If $\overline{C}_\theta + \widehat{T}_{\text{RCSP}}(i, Q - q_\theta) \geq 0$, then the label extension has non-negative reduced cost, i.e., $\overline{C}_{\theta'} \geq 0$.*

Proof. We provide proof for the RCSP bound in Appendix C. □

Knapsack Bound. Consider a label L_θ representing a route θ that ends at customer i . We build a $\{0, 1\}$ -knapsack problem with N items and capacity $Q - q_\theta$. We associate a weight $w_j = q_j$ to each item $j \in \{1, \dots, N\}$, equal to the demand of customer $j \in \mathcal{V} \setminus \{0\}$, and a value consisting of the dual value γ_j minus a lower bound on the average penalty:

$$v_{ij}(\theta) = \gamma_j - \pi(\tau_\theta + \min_{\omega \in \Omega} t_{ij}^\omega - \ell_j), \quad (22)$$

such that the following inequality holds:

$$-v_{ij}(\theta) \leq \sum_{\omega \in \Omega} \alpha^\omega \cdot \pi(a_{\theta \oplus (i,j)}(j; \mathbf{t}^\omega) - \ell_j) - \gamma_j. \quad (23)$$

We can express the knapsack problem as an integer linear program:

$$\max \quad \sum_{j \in \mathcal{V} \setminus \{0\}} v_{ij}(\theta) z_j \quad (24)$$

$$\text{s.t.} \quad \sum_{j \in \mathcal{V} \setminus \{0\}} q_j z_j \leq Q - q_\theta \quad (25)$$

$$z_j = 0 \text{ if } j \in \theta \quad \forall j \in \mathcal{V} \setminus \{0\} \quad (26)$$

$$z_j \in \{0, 1\} \quad \forall j \in \mathcal{V} \setminus \{0\} \quad (27)$$

where Constraints (26) enforce that item j is considered for inclusion in the knapsack only if it is not already in route θ . Let \mathbf{z}^* be an optimal solution to the $\{0, 1\}$ -knapsack problem and let $\bar{\mathbf{z}}$ be a solution to its linear relaxation. Then, we define the following completion bound:

$$\widehat{T}_{ks}(i, Q - q_\theta) = - \sum_{j \in \mathcal{V} \setminus \{0\}} v_{ij}(\theta) \bar{z}_j. \quad (28)$$

Proposition 2 *Let θ be a route starting at the depot and ending at customer i with reduced cost \bar{C}_θ and cumulative demand q_θ . Let $L_{\theta'}$ be a label extension associated with the route $\theta' = \theta \oplus \mathcal{E}$, where $\mathcal{E} = (u_1, u_2, \dots, u_L)$ is a path such that $u_j \notin \theta, \forall u_j \in \mathcal{E}$, and $q_{\theta'} \leq Q$. If $\bar{C}_\theta + \widehat{T}_{ks}(i, Q - q_\theta) \geq 0$, then the label extension has non-negative reduced cost, i.e., $\bar{C}_{\theta'} \geq 0$.*

Proof. We provide proof for the knapsack bound in Appendix C. □

4.3. Column Generation for Penalty-based Approximation

We now describe how the column generation (CG) approach from the previous sections can be modified to solve the penalty-based approximation of Model (L). The RMP for the penalty-based model optimizes the objective function:

$$\min_{\theta \in \Theta} \hat{f}_{\theta'}(\mathbf{z}, \mathbf{x}), \quad (\text{RMP-L})$$

while the constraints remain the same as in (RMP). Accordingly, we incorporate the late arrival penalty prediction model into the pricing problem:

$$\min_{\theta \in \Theta} \bar{C}_{\theta} \triangleq C_{\theta} + \sum_{i \in \theta} h(\mathbf{f}(\mathbf{x}^{n+1}, \theta, i); \mathbf{H}) - \sum_{i \in \theta} \gamma_i - \mu. \quad (\text{PP-L})$$

To solve the pricing problem in (PP-L), we make the following modifications to the labeling algorithm described in Section 4.2. First, when extending a label L_{θ} along an arc (i, j) , we generate a new path θ' with a reduced cost given by:

$$\bar{C}_{\theta'} = \bar{C}_{\theta} - c_{i0} + c_{ij} + c_{j0} + h(\mathbf{f}(\mathbf{x}^{n+1}, \theta', j); \mathbf{H}) - \gamma_j, \quad (29)$$

where we replace the sample averaged penalty in Equation (18) by the predicted penalty.

Second, we cannot define the earliest service start time τ_{θ} as in Equation (17) since we do not assume a set of scenarios to be available under the penalty-based approximation model. Instead, we rely on the following assumption to compute τ_{θ} :

Assumption 1 (Earliest Arrival Times) *Given a route θ , it holds that*

$$a_{\theta}(i; \tilde{\mathbf{t}}) \geq \min_{k \in \{1, \dots, n\}} a_{\theta}(i; \mathbf{t}^k) \quad \forall i \in \theta.$$

Assumption 1 states that, for a given route θ , any realization of the vector of travel times will lead to an arrival time at customer $i \in \theta$ that is not earlier than the most optimistic arrival time that one would observe given the historical travel times $\{\mathbf{t}^k\}_{k \in \{1, \dots, n\}}$ from the training data set \mathbf{T} . In practice,

there often exists periods in which highways have no traffic and cars can travel at free flow, e.g., during quiet night hours. We argue that Assumption 1 is reasonable if the historical data contains travel time observations recorded at such periods with low traffic. Even if the historical data does not contain such observations, our assumption is not limiting as one can always augment the data set with artificial scenarios by computing free-flow travel times for each arc. Given the above assumption, we define the earliest service start time:

$$\tau_\theta = \min_{k \in \{1, \dots, n\}} \left\{ s_\theta(i, \mathbf{t}^k) \right\}, \quad (30)$$

which is independent of the penalty prediction model $h(\cdot)$. We run the pricing algorithm from Section 4.2 with the above modifications to solve (PP-L).

5. Design of Experiments

The goals of our experiments are to (i) compare different data-driven methods for the CS-VRPTW, based on the average cost calculated on a test data set containing travel times and features, (ii) analyze the value of incorporating features in the VRPTW, and (iii) investigate the performance of the proposed methods under different generative models for travel times and features.

We implemented the BP&C method in C++, using CPLEX as the underlying linear programming solver. All experiments were conducted on the Narval computing cluster from the Digital Research Alliance of Canada, Canada’s national high-performance computing system. We set a time limit of 5 hours per run. We provide the source code and data to reproduce our experiments at [to be disclosed after peer-review].

5.1. Instances

We base our experiments on the instances of Solomon (1987), a standard benchmark for the VRPTW. Each instance describes a graph $\mathcal{G} = (\mathcal{V}, \mathcal{A})$, a vehicle capacity Q , demands q_i and time windows $[e_i, \ell_i]$ of each node $i \in \mathcal{V}$, with the demand for the depot being equal to zero. We define

the deterministic cost c_{ij} to be the Euclidean distance between each pair of customers $(i, j) \in \mathcal{A}$, and assume a quadratic penalty function, i.e., $\pi(u) = u^2$ for $u \geq 0$.

We adopted 29 instances from problem sets R1, C1, and RC1, which have short time windows, allowing only a few customers per route. Problem set R1 contains randomly generated geographical data, C1 contains clustered data, and RC1 has a mix of random and clustered structures.

For each instance, we generate synthetic historical data $\mathbf{X} \in \mathbb{R}^{n \times p}$ and $\mathbf{T} \in \mathbb{R}^{n \times |\mathcal{A}|}$ with $n = 100$ training travel time scenarios and $p = 10$ features. We selected the values for n and p reflecting, e.g., a typical VRP application in city logistics where one might have daily observations of features and average travel times for a certain period of the day. For each $k \in \{1, \dots, n\}$, we sample a feature vector from a p -variate distribution $\mathbf{x}^k \sim \mathbb{X}$ and we sample travel times from an $|\mathcal{A}|$ -variate distribution $\mathbf{t}^k \sim \mathbb{T}(\mathbf{x}^k)$ conditioned on the observed feature vector \mathbf{x}^k . We consider three different generative models, which specify the distributions \mathbb{X} and \mathbb{T} .

Linear model. For each arc $(i, j) \in \mathcal{A}$, the deterministic cost c_{ij} defines a nominal travel time \underline{t}_{ij} corresponding to the free-flow travel time of the arc. We define the stochastic travel times as the nominal travel times $\underline{\mathbf{t}} = [\underline{t}_{ij}]_{(i,j) \in \mathcal{A}}$ plus a random noise term which depends linearly on the features:

$$\tilde{\mathbf{t}}_{\text{linear}}(\tilde{\mathbf{x}}) = \underline{\mathbf{t}} + \mathbf{B}^\top \tilde{\mathbf{x}} + \tilde{\boldsymbol{\varepsilon}} \quad (31)$$

where \mathbf{B} is a $p \times |\mathcal{A}|$ matrix whose columns are given by the vectors $\mathbf{b}_{ij} \in \mathbb{R}^p$ for $(i, j) \in \mathcal{A}$. We sample values in \mathbf{b}_{ij} from a uniform distribution with support ranging from 1% to 20% of the corresponding nominal travel time $\underline{t}_{ij} = c_{ij}$. Moreover, we assume that features are binary, $\mathbf{x} \in \{0, 1\}^p$, corresponding to categorical data, e.g., day of the week, holidays, or roadworks. The noise term $\tilde{\boldsymbol{\varepsilon}}$ follows a multivariate normal distribution with zero mean, and covariance matrix generated according to the method of Rostami et al. (2021), such that noise values at different arcs are correlated. Lastly, we assume that travel times on each arc must be greater than or equal to the nominal travel time, and we truncate

travel times whenever necessary.

Exponential model. For each arc $(i, j) \in \mathcal{A}$, we consider that features are related to the travel times via an exponential function:

$$\tilde{t}_{ij} = \underline{t}_{ij} + 0.2 \underline{t}_{ij} \exp(2 \mathbf{b}_{ij}^\top \tilde{\mathbf{x}}) + \tilde{\varepsilon}_{ij} \quad (32)$$

where features now follow a uniform distribution between 0 and 1. We generate the parameter vectors $\mathbf{b}_{ij} \in \mathbb{R}^p$ by sampling each element from a uniform distribution between 0.1 and 0.3, and we multiply each element by -1 with a probability of 0.2. Due to the exponential travel times, having normally distributed $\tilde{\varepsilon}_{ij}$ does not provide sufficient noise. Therefore, we assume that $\tilde{\varepsilon}_{ij}$ follows a log-normal distribution with zero mean and standard deviation $\sigma_\varepsilon = 1$.

Sigmoidal model. For each arc $(i, j) \in \mathcal{A}$, we generate travel times:

$$\tilde{t}_{ij} = \underline{t}_{ij} + \underline{t}_{ij} \sigma\left(32\left(\frac{1}{2} \mathbf{b}_{ij}^\top \mathbb{1} - \mathbf{b}_{ij}^\top \tilde{\mathbf{x}}\right)\right) + \tilde{\varepsilon}_{ij} \quad (33)$$

where $\sigma(x) = 1/(1 + e^{-x})$ is the sigmoid function. Features follow a uniform distribution between 0 and 1. The noise term $\tilde{\varepsilon}_{ij}$ follows a log-normal distribution with mean 0 and standard deviation $\sigma_\varepsilon = 1.2$. We generate the parameter vectors \mathbf{b}_{ij} by sampling each element from a uniform distribution between 0.3 and 0.8, and we multiply each element by -1 with a probability of 0.2. Due to its characteristic shape, we can interpret the sigmoidal model as representing two feature-dependent *states of traffic*, e.g., a congested and a non-congested state.

5.2. Prescriptive Metrics

We use the term *prescription* to refer to any function $\hat{\mathbf{z}}(\mathbf{x})$ that provides a decision given the feature observation $\tilde{\mathbf{x}} = \mathbf{x}$. We evaluate the performance of a given prescription $\hat{\mathbf{z}}(\cdot)$ by its expected cost under the true joint distribution of travel times and features:

$$R(\hat{\mathbf{z}}) = \mathbb{E}_{\tilde{\mathbf{x}} \sim \mathbb{X}} \left[\mathbb{E}_{\tilde{\mathbf{t}} \sim \mathbb{T}} [f_\Theta(\hat{\mathbf{z}}(\mathbf{x}), \tilde{\mathbf{t}}) \mid \tilde{\mathbf{x}} = \mathbf{x}] \right] \quad (34)$$

In practice, calculating the above expectation is often intractable. We therefore estimate $R(\hat{\mathbf{z}})$ using a test data set, which we construct by sampling a set $\mathcal{X} = \{\mathbf{x}^k \sim \mathbb{X}\}_{k=1, \dots, n_{\mathcal{X}}}$ of features and, for each feature vector $\mathbf{x} \in \mathcal{X}$, a set $\mathcal{T}(\mathbf{x}) = \{\mathbf{t}^k \sim \mathbb{T}(\mathbf{x})\}_{k=1, \dots, n_{\mathcal{T}}}$ of travel times from the corresponding generative model. The empirical *test cost* $\hat{R}(\hat{\mathbf{z}})$ of a prescription $\hat{\mathbf{z}}(\cdot)$ is an approximation of $R(\hat{\mathbf{z}})$ which is given by:

$$\hat{R}(\hat{\mathbf{z}}) = \frac{1}{n_{\mathcal{X}} \cdot n_{\mathcal{T}}} \sum_{\mathbf{x} \in \mathcal{X}} \sum_{\mathbf{t} \in \mathcal{T}(\mathbf{x})} f_{\Theta}(\hat{\mathbf{z}}(\mathbf{x}), \mathbf{t}). \quad (35)$$

In Section 6, we provide test cost results for prescriptions based on different models, where we replace $\hat{\mathbf{z}}$ in Equation (35) by the solution to the corresponding model.

5.3. Full-information benchmarks

We compare our models against benchmark solutions that rely on knowledge of travel times and feature distributions. The following benchmark solutions are impractical in a real-world setting, as the decision-maker does not know the underlying distributions. However, these benchmark solutions provide us with a relative measure of how well the proposed practical models perform.

Full-information solution. Based on the test data set, we can approximate the full-information solution of the CS-VRPTW, given a feature vector $\mathbf{x} \in \mathcal{X}$, as:

$$\hat{\mathbf{z}}_{\text{FULL}}^*(\mathbf{x}) = \arg \min_{\mathbf{z} \in \mathcal{Z}_{\Theta}} \frac{1}{n_{\mathcal{T}}} \sum_{\mathbf{t} \in \mathcal{T}(\mathbf{x})} f_{\Theta}(\mathbf{z}, \mathbf{t}), \quad (36)$$

with optimal objective value:

$$\hat{v}_{\text{FULL}}^*(\mathbf{x}) = \min_{\mathbf{z} \in \mathcal{Z}_{\Theta}} \frac{1}{n_{\mathcal{T}}} \sum_{\mathbf{t} \in \mathcal{T}(\mathbf{x})} f_{\Theta}(\mathbf{z}, \mathbf{t}). \quad (37)$$

Given the prescription $\hat{\mathbf{z}}_{\text{FULL}}^*$, the empirical test cost is given by:

$$\hat{R}_{\text{FULL}} = \hat{R}(\hat{\mathbf{z}}_{\text{FULL}}^*) = \frac{1}{n_{\mathcal{X}} \cdot n_{\mathcal{T}}} \sum_{\mathbf{x} \in \mathcal{X}} \sum_{\mathbf{t} \in \mathcal{T}(\mathbf{x})} f_{\Theta}(\hat{\mathbf{z}}_{\text{FULL}}^*(\mathbf{x}), \mathbf{t}) = \frac{1}{m_{\mathcal{X}}} \sum_{\mathbf{x} \in \mathcal{X}} \hat{v}_{\text{FULL}}^*(\mathbf{x}), \quad (38)$$

which provides a lower bound for the empirical test cost of any model. With this definition, we calculate

the full-information percentage gap of a prescription $\hat{\mathbf{z}}$ as:

$$\rho(\hat{\mathbf{z}}) = \frac{\hat{R}(\hat{\mathbf{z}}) - \hat{R}_{\text{FULL}}}{\hat{R}_{\text{FULL}}}. \quad (39)$$

Predict with full information, then optimize. The performance of a prescription under the PTO framework depends on the choice of predictive model $\mathbf{g}(\cdot)$ providing travel time predictions $\hat{\mathbf{t}} = \mathbf{g}(\mathbf{x}; \boldsymbol{\varphi})$. For the purpose of benchmarking, we define the PTO-F problem, which assumes that the predictive model perfectly predicts the expected travel times given observed features:

$$\mathbf{z}_{\text{PTO-F}}^*(\mathbf{x}) = \arg \min_{\mathbf{z} \in \mathcal{Z}_{\Theta}} f_{\Theta}(\mathbf{z}, \bar{\mathbf{t}}) \quad \text{with } \bar{\mathbf{t}} = \mathbb{E}[\tilde{\mathbf{t}} \mid \tilde{\mathbf{x}} = \mathbf{x}]. \quad (40)$$

A solution for the PTO-F problem requires knowledge of the joint distribution of travel times and features. We can approximate the PTO-F solution using the test data set:

$$\hat{\mathbf{z}}_{\text{PTO-F}}^*(\mathbf{x}) = \arg \min_{\mathbf{z} \in \mathcal{Z}_{\Theta}} f_{\Theta}(\mathbf{z}, \hat{\mathbf{t}}) \quad \text{with } \hat{\mathbf{t}} = \frac{1}{n_{\mathcal{T}}} \sum_{\mathbf{t} \in \mathcal{T}(\mathbf{x})} \mathbf{t}. \quad (41)$$

We note that although PTO-F often performs better than PTO with practical prediction models, PTO-F does not necessarily provide a lower bound for PTO regarding test cost since neither PTO nor PTO-F account for the structure of the downstream optimization problem. Specifically, the true conditional expected travel times do not necessarily correspond to the travel times leading to minimum cost.

5.4. Prescriptive methods

We compare the ten prescriptive methods summarized in Table 1. The top eight methods are derived from the data-driven prescriptive models of Section 3 and correspond to practical methods for solving the CS-VRPTW. The bottom two prescriptive methods are full-information benchmarks, included for comparison, and cannot be applied in practice as they require knowledge of the true travel times distribution (see Section 5.3).

D-avg is the point-based model under average travel times based on historical data. PTO-OLS is the point-based model under the PTO framework, where the coefficients $\boldsymbol{\varphi} \in \mathbb{R}^{|\mathcal{A}| \times p}$ of the prediction

Table 1: Data-driven prescriptive methods (top) and full-information benchmarks (bottom).

Method	Model	Description
D-avg	(P)	Predicted travel times given by average travel times $\hat{\mathbf{t}} = \sum_{k=1}^n \mathbf{t}^k / n$
PTO-OLS	(P)	Predicted travel times $\hat{\mathbf{t}} = \boldsymbol{\varphi} \mathbf{x}^{n+1}$ using OLS regression (predict-then-optimize)
PTO- k NN	(P)	Predicted travel times $\hat{\mathbf{t}}$ given by k -NN regression (predict-then-optimize)
SAA	(S)	Travel time scenarios are the set of historical travel times $\Omega = \{\mathbf{t}^1, \dots, \mathbf{t}^n\}$ with $\alpha^\omega = 1/n$
SAA- k NN	(S)	Historical travel times with weights α^ω given by k -NN regression (Bertsimas and Kallus 2019)
CSAA	(S)	Feature-dependent travel time scenarios (see Section 3.3)
RSAA	(S)	Feature-dependent travel time scenarios based on linear regression residuals (see Section 3.4)
P-NN	(L)	Penalty prediction model based on fully-connected neural network
PTO-F	(P)	Predict-then-optimize under true conditional expected travel times $\hat{\mathbf{t}} = \mathbb{E}_{\mathbf{t} \sim \mathbb{T}}[\mathbf{t} \mathbf{x}^{n+1}]$
Full	(S)	Full-information lower bound under the true travel times distribution $\mathbf{t} \sim \mathbb{T}(\mathbf{x}^{n+1})$

model are trained by solving a multiple least squares regression on the historical data. PTO- k NN is the point-based model under the PTO framework, where we used a k -nearest neighbor regression model to predict the travel times. The SAA model assumes that the travel time scenarios are given by the historical travel times. SAA- k NN corresponds to the approach of Bertsimas and Kallus (2019), where we adopted a k -nearest neighbors regression model for the weight function. As described in Section 3.3, CSAA generates a set of travel time scenarios Ω from a multivariate Gaussian distribution with mean and covariance given by $\hat{\mathbf{B}}^\top \mathbf{x}^{n+1}$ and $\hat{\boldsymbol{\Sigma}}$, respectively. RSAA generates a set of travel time scenarios Ω based on the residuals of a linear regression model trained on historical data. P-NN is the penalty-based approximation model in which the late arrival penalty prediction model is a fully-connected neural network with two hidden layers with 100 neurons each, trained with the Adam optimization algorithm to minimize the squared error loss with an ℓ_2 regularization term equal to 0.1. Note that methods D-avg and SAA ignore the features and only consider the historical travel times when searching for a solution for the current period $n + 1$.

6. Computational Results

We start our analysis with a small example illustrating the benefit of incorporating information from feature data in the VRPTW formulation, which eases the reader to develop an intuition why feature-based approaches can yield results superior to feature-agnostic approaches. We then report results on larger instances, where we discuss the test cost performance of the different prescriptive methods.

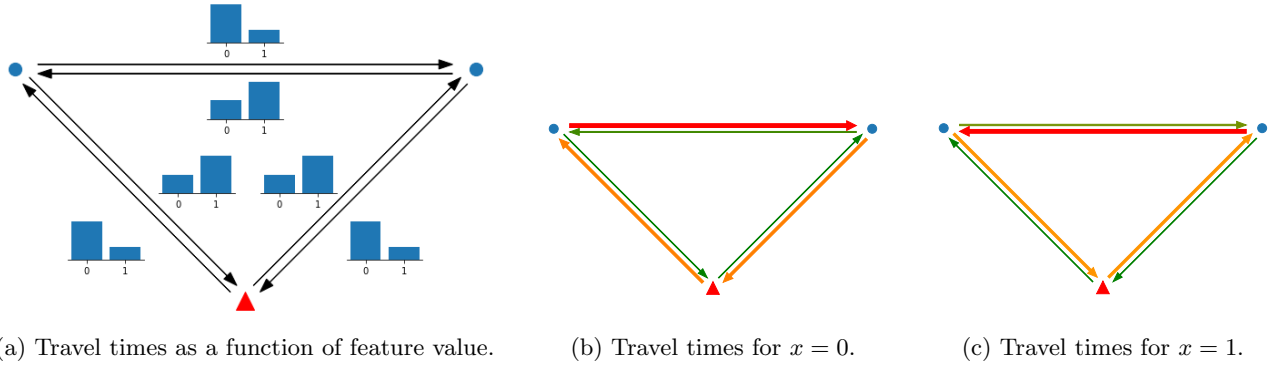
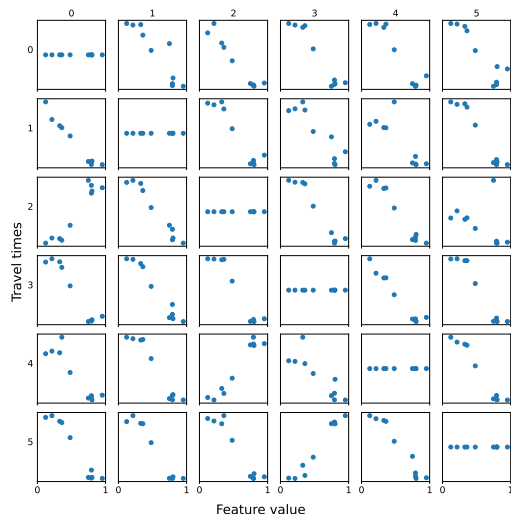


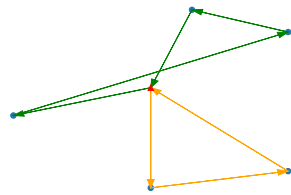
Figure 1: Joint distribution and different realizations of travel times and feature variable.

6.1. Illustrative example

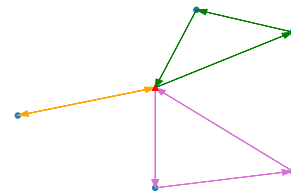
We consider a network with $N = 2$ customers and a training data set with $n = 2$ samples and $p = 1$ binary feature. Figure 1a shows the customer locations and arcs connecting each pair of customers. A small bar chart next to each arc shows the corresponding travel times in the y-axis as a function of the feature value in the x-axis. We omitted the values in the y-axis since this illustrative example is not concerned with specific travel time values but rather aims to show the relation between travel times and features. Figure 1b and 1c show the two possible scenarios, representing travel time realizations when the feature value equals $x = 0$ and $x = 1$, respectively. The color and line thickness of each arc indicate the amount of congestion, with thicker lines representing more congestion, and different colors indicating whether the arc is strongly congested (red), mildly congested (orange), or free from congestion (green). Under the scenario displayed in Figure 1b, a route that starts at the depot and visits customers in a clockwise direction will experience more congestion than a counter-clockwise route. Therefore, if the decision-maker finds herself in a scenario where $x = 0$, following the counter-clockwise route is optimal. Figure 1c shows the reverse pattern, i.e., when $x = 1$, the counter-clockwise route is more congested than the clockwise route. Existing methods based on SAA, which are widely adopted in the field, would provide a clockwise route that is optimal when $x = 0$ but not when $x = 1$. In contrast to featureless methods, feature-dependent solutions for the CS-VRPTW can provide the optimal route in both cases.



(a) Relation between travel times and features in the training data set for each arc.



(b) Solution structure A.



(c) Solution structure B.

Feature re- alization	D-avg	SAA	CSAA	Full
$x = 0.28$	A	B	A	A
$x = 0.83$	A	B	B	B

(d) Optimal solution structures of each method.

Figure 2: Data set and solution structures of our illustrative example.

We now extend our previous example and consider a network with $N = 5$ customers and a training data set with $n = 10$ samples and $p = 1$ continuous feature with domain $x \in [0, 1]$. To capture different degrees of congestion, we assume sigmoidal travel times (see Section 5.1). In Figure 2a, each scatter plot in row $i \in \{0, \dots, 5\}$ and column $j \in \{0, \dots, 5\}$ shows the travel times and features in the training data set corresponding to arc $(i, j) \in \mathcal{A}$. For a more palatable exposition, we normalized the travel times of each arc based on its nominal free-flow travel time. We compare the optimal solutions of two featureless prescriptive methods, i.e., D-avg and SAA, against CSAA and full-information solutions. Figures 2c and 2b show the solution structures that emerge in our example. Note how the solution structures are fundamentally different from each other. In particular, Solution A requires three vehicles, while Solution B requires only two vehicles. In Figure 2d, we show the solution structures obtained by each method under different realizations of the feature variable. When $x = 0.28$, the featureless point-based approximation (D-avg) retrieves the full-information solution, but it fails to do so when $x = 0.83$. We see the opposite behavior for the featureless SAA method, i.e., it fails for $x = 0.28$ but can retrieve the full-information solution when $x = 0.83$. In contrast to the featureless approaches, CSAA provides feature-dependent solutions that match the full-information solution in both cases. This small example

shows that ignoring information from feature data can lead to suboptimal solutions, underlying the benefit of the proposed CS-VRPTW formulation.

6.2. Results

We analyze the suitability of the different prescriptive methods in solving the CS-VRPTW. Specifically, we investigate the performance of each method in terms of their test cost \hat{R} and full-information percentage gaps ρ . To provide a meaningful comparison of the prescriptive methods, we only consider instances for which all methods could find a near-optimal solution with an optimality gap of at most 1%. We restrict the discussion in the subsequent analyses to instances with 25 and 50 customers, for which we obtained a reasonably large set of near-optimal solutions. We provide detailed results for instances with 25 and 50 customers in Appendix D and Appendix E, respectively. We focus on larger instances with 75 and 100 customers in Section 6.3, where we study the scalability of the BP&C algorithm. As we later discuss, the P-NN method has longer run times and could not solve many instances with 50 customers. Therefore, we show results for P-NN only for instances with 25 customers.

Average test cost performance. Table 3 summarizes the test cost performance of all methods, showing the full-information percentage gap of test costs averaged over all instances with a common number of customers N , generative model, and instance type. In the last column, we show the absolute test cost values of the full-information benchmark. Among the data-driven prescriptive methods, we highlight the lowest values on each row with boldface numbers.

In most settings, CSAA and RSAA achieve the lowest test costs among the data-driven prescriptive methods. In particular, they outperform the PTO-F benchmark, even though PTO-F has an unfair advantage of having access to the full distribution. As discussed in previous works (cf. Bertsimas and Kallus 2019, Elmachtoub and Grigas 2021), travel time predictions minimizing a least squares deviation may not lead to optimal decisions since they do not account for the structure of the optimization objective. In line with previous works, our results show that PTO-F often finds suboptimal decisions

Table 3: Overview of average test costs for different instance types and generative models.

N	Gen. model	Inst. type	D-avg	SAA	PTO-OLS	PTO- k NN	SAA- k NN	CSAA	RSAA	P-NN	PTO-F	Full (Abs.)
25	Lin.	R	23.42	3.38	0.97	11.00	4.25	0.06	0.11	0.59	0.99	483.19
		C	0.00	0.00	0.00	0.00	0.48	0.00	0.00	0.14	0.00	192.66
		RC	17.32	6.00	2.97	16.48	3.14	0.42	0.38	2.56	2.11	374.16
	Exp.	R	65.10	15.07	3.71	15.73	6.37	2.24	2.07	2.54	2.18	624.45
		C	44.37	3.98	12.67	42.28	8.52	2.82	3.47	2.16	7.94	220.52
		RC	99.82	24.70	13.24	34.30	10.53	7.75	9.58	10.52	6.03	514.96
	Sig.	R	97.60	19.10	39.06	58.83	18.95	13.70	12.89	23.03	16.96	612.18
		C	85.70	30.37	74.45	72.38	45.89	41.00	42.48	47.35	81.26	231.30
		RC	233.19	31.12	89.02	120.53	34.35	32.77	37.99	52.42	49.80	516.79
50	Lin.	R	23.49	4.14	2.06	14.20	3.47	0.38	0.31	-	1.33	917.0
		C	1.14	5.22	0.49	1.14	0.89	0.16	0.16	-	0.49	369.6
		RC	55.09	5.76	4.87	23.38	7.84	0.71	0.64	-	3.69	896.9
	Exp.	R	49.12	13.31	6.96	13.75	6.27	3.67	4.34	-	3.76	1171.4
		C	45.44	10.37	5.25	30.75	3.42	2.89	2.36	-	5.21	432.2
		RC	82.81	34.14	22.35	25.20	28.06	6.19	9.63	-	4.80	1274.0
	Sig.	R	191.73	34.13	67.16	95.00	32.86	24.37	26.51	-	27.82	1229.0
		C	105.19	23.49	62.00	67.45	28.58	34.54	29.78	-	46.55	451.3
		RC	303.64	49.66	101.90	157.20	54.73	44.97	48.50	-	35.49	1413.9

despite using the true expected travel times under full distributional information.

Analysis of test cost distributions. We focus on the distribution of test costs for instances with 25 customers. Figure 3 presents full-information gaps of each method, summarized as boxplots with whiskers that extend to 1.5 times the interquartile range. Points outside this range are marked as outliers and noted with an “ \times ”.

We first note that, as expected, CSAA and RSAA have the smallest gaps for instances with linear travel times, as the data in this case conforms with the model assumptions. Second, we observe that P-NN provides competitive solutions in general and, especially for instances with exponential travel times, often outperforms all other methods. In particular, P-NN often improves upon PTO-based methods, highlighting the advantage of directly predicting the late arrival penalty rather than relying on travel time predictions. Still, CSAA and RSAA present equal or even superior performance in this non-linear setting. Third, for instances with sigmoidal travel times, we observe that SAA-based methods, i.e., SAA- k NN, CSAA, RSAA, and the classical SAA, have the smallest full-information gaps. In this highly non-linear setting, we benefit from using scenarios that better capture travel time

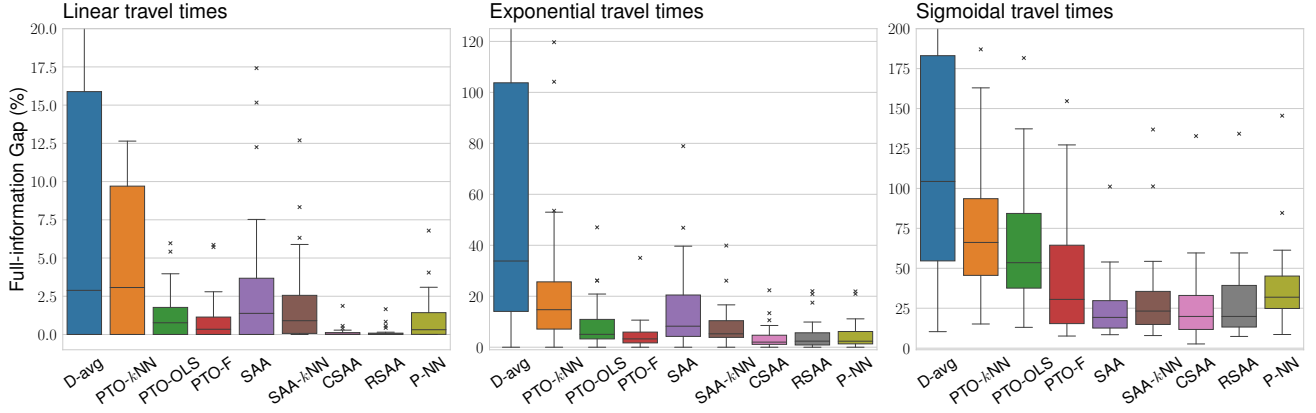


Figure 3: Distribution of test costs for instances with 25 customers from different generative models.

variability, as illustrated in our example in Section 6.1. In general, we conclude that simpler methods that extend SAA using feature-dependent scenarios are the most promising, providing solutions that are closest to the full-information benchmark. Although it might be surprising that CSAA and RSAA can outperform the more sophisticated P-NN method, we argue that predicting late arrival penalties is not straightforward because the training data set must reflect the relation between the different combinatorial structures, encoded in the projected features, and the resulting penalty. The proposed penalty prediction model is not always capable of learning all the combinatorial intricacies of the VRP problem.

Trade-offs between first and second-stage costs. We analyze the contributions of the first-stage and second-stage costs to the total test cost. Figure 4 displays the average test cost of each method for instances with an exponential generative model, where we decompose the test cost $\hat{R}(\hat{\mathbf{z}})$ of a solution as the sum of the first-stage cost \hat{C} and the second-stage cost \hat{Q} :

$$\hat{R}(\hat{\mathbf{z}}) = \frac{1}{n_{\mathcal{X}} \cdot n_{\mathcal{T}}} \sum_{\mathbf{x} \in \mathcal{X}} \sum_{\mathbf{t} \in \mathcal{T}(\mathbf{x})} C(\hat{\mathbf{z}}) + Q(\hat{\mathbf{z}}, \mathbf{t}) = \hat{C}(\hat{\mathbf{z}}) + \hat{Q}(\hat{\mathbf{z}}). \quad (42)$$

The top, middle, and bottom plots show results for instances of types R, C, and RC, respectively. Full-information solutions have first-stage costs that are often larger than those of other methods, showing that it is often beneficial to incur larger first-stage costs and compensate them with comparatively

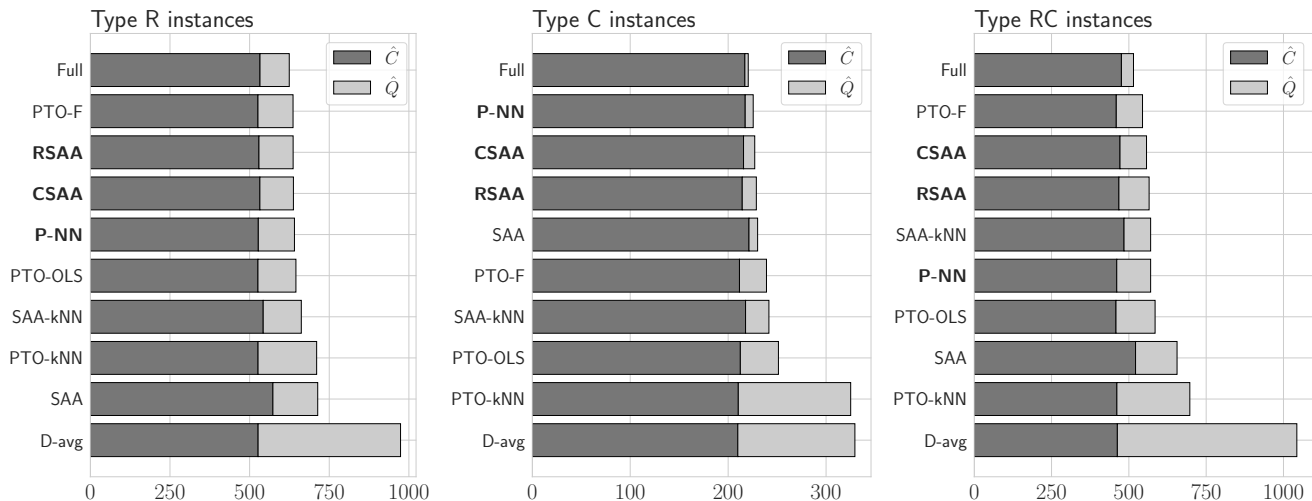


Figure 4: Average first-stage and second-stage test costs for instances from the exponential generative model.

small late arrival penalties. On the contrary, optimizing for the first-stage cost can lead to solutions with large penalties and, consequently, large overall test costs, as we see, e.g., in the middle plot for the D-avg method. Compared to practical PTO methods, i.e., PTO-OLS and PTO- k NN, our proposed CSAA and P-NN methods often present larger first-stage costs but smaller total test costs, bearing more similarity to the results from the full-information benchmark.

6.3. Scaling to larger instances

Figure 5 compares the solution times of the different methods. For this plot, we considered all instances with 25 customers and a linear generative model. We observe that P-NN shows the longest run times, followed by SAA and the full-information benchmark. Recall that we solve all methods using the BP&C algorithm described in Section 4. Specifically for the P-NN method, we adopt the modified pricing problem described in Section 4.3. Consequently, with the exception of the P-NN method, the solution algorithms to all data-driven models differ only in the specific travel time scenarios given as input to the BP&C algorithm.

Figure 6 shows how solution times increase as we increase the number of customers. Here, we focus on the CSAA method and consider instances with a linear generative model. With 25 customers, we

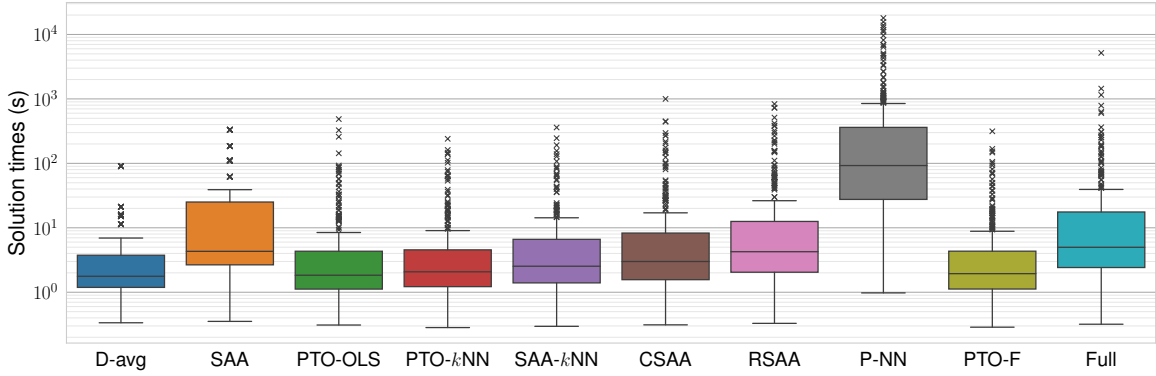


Figure 5: Solution times of different methods for instances with 25 customers with a linear generative model.

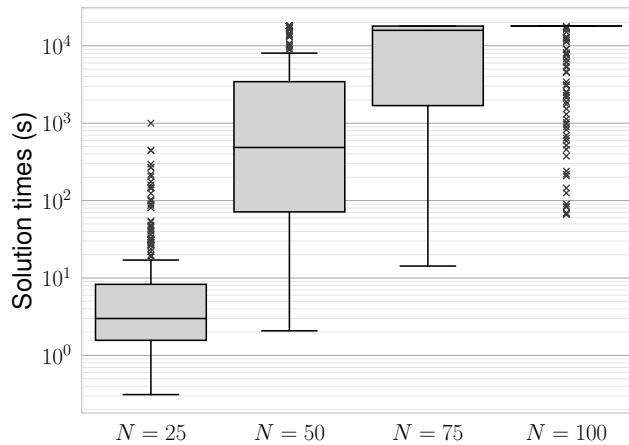


Figure 6: Solution times of the CSAA method for increasing number of customers on instances with a linear generative model.

can solve most instances in less than 10 seconds. Due to the \mathcal{NP} -hardness of the problem, solution times increase drastically, and we observe some runs reaching the 5-hour time limit already with 50 customers. With 100 customers, we can only solve very few instances within the time limit.

7. Conclusions

This work connects the recent literature on contextual optimization with the established research field of VRPs. We introduced a novel formulation incorporating contextual information into the stochastic VRPTW. To solve the proposed formulation, we derived several data-driven prescriptive models by (i) applying existing contextual optimization methods to our problem setting and (ii) proposing novel methods based on conditional SAA and penalty-based prediction. From a computational perspective,

solving the VRPTW is a challenging task for which many solution techniques exist in the literature. We showed how state-of-the-art techniques can be adapted when contextual information is available, leading to a customized BP&C algorithm that can solve instances with up to 100 customers. We analyzed the out-of-sample cost performance of the data-driven methods. We observed that the penalty-based approximation model that relies on penalty predictions provides competitive solutions, but in general, an SAA method based on feature-dependent scenarios yields solutions that are closest to the full-information benchmark.

This work raises several possibilities for future research. First, although we studied various data-driven methods and compared them against different benchmarks, we certainly did not exhaustively explore all possible approaches for solving the CS-VRPTW. Future research could investigate variations of the presented methods, e.g., the use of non-linear probabilistic models within the CSAA approach, or propose novel models and algorithms. Second, while extending the presented techniques to some VRP variants might be straightforward, e.g., with stochastic service times, other problem variants could lead to more interesting research problems. Finally, since this paper focused on modeling aspects and exact solution methods, one open question is how to adapt existing heuristic methods to harness contextual information to efficiently solve larger instances.

Acknowledgments

This research has been funded by the Deutsche Forschungsgemeinschaft (DFG, German Research Foundation) as part of the research group Advanced Optimization in a Networked Economy (AdONE, GRK2201/277991500). This support is gratefully acknowledged. This research was enabled in part by support provided by Calcul Québec (<https://www.calculquebec.ca/>) and the Digital Research Alliance of Canada (<https://alliancecan.ca>).

References

- Adulyasak Y, Jaillet P (2016) Models and algorithms for stochastic and robust vehicle routing with deadlines. *Transportation Science* 50(2):608–626.
- Ban GY, Gallien J, Mersereau AJ (2019) Dynamic procurement of new products with covariate information: The residual tree method. *Manufacturing & Service Operations Management* 21(4):798–815.
- Ban GY, Rudin C (2019) The big data newsvendor: Practical insights from machine learning. *Operations Research* 67(1):90–108.
- Barnhart C, Johnson EL, Nemhauser GL, Savelsbergh MWP, Vance PH (1998) Branch-and-price: Column generation for solving huge integer programs. *Operations Research* 46(3):316–329.
- Bertsimas D, Kallus N (2019) From predictive to prescriptive analytics. *Management Science* 66(3):1025–1044.
- Bertsimas D, McCord C (2018) Optimization over continuous and multi-dimensional decisions with observational data. Bengio S, Wallach H, Larochelle H, Grauman K, Cesa-Bianchi N, Garnett R, eds., *Advances in Neural Information Processing Systems*, volume 31 (Curran Associates, Inc.).
- Bertsimas D, McCord C (2019) From predictions to prescriptions in multistage optimization problems. *arXiv preprint arXiv:1904.11637* .
- Bertsimas D, McCord C, Sturt B (2023) Dynamic optimization with side information. *European Journal of Operational Research* 304(2):634–651.
- Beutel AL, Minner S (2012) Safety stock planning under causal demand forecasting. *International Journal of Production Economics* 140(2):637–645.
- Costa L, Contardo C, Desaulniers G (2019) Exact branch-price-and-cut algorithms for vehicle routing. *Transportation Science* 53(4):946–985.
- Dabia S, Ropke S, Van Woensel T, De Kok T (2013) Branch and price for the time-dependent vehicle routing problem with time windows. *Transportation Science* 47(3):380–396.
- Elmachtoub AN, Grigas P (2021) Smart “predict, then optimize”. *Management Science* 68(1):9–26.
- Errico F, Desaulniers G, Gendreau M, Rei W, Rousseau LM (2018) The vehicle routing problem with hard time windows and stochastic service times. *EURO Journal on Transportation and Logistics* 7(3):223–251.
- Florio A, Hartl R, Minner S (2020) New exact algorithm for the vehicle routing problem with stochastic demands. *Transportation Science* 54(4):1073–1090.
- Gendreau M, Ghiani G, Guerriero E (2015) Time-dependent routing problems: A review. *Computers & Operations Research* 64:189–197.
- Gendreau M, Jabali O, Rei W (2014) Chapter 8: Stochastic vehicle routing problems. *Vehicle Routing: Problems, Methods, and Applications, Second Edition*, 213–239 (SIAM).
- Ghosal S, Ho CP, Wiesemann W (2021) A unifying framework for the capacitated vehicle routing problem under risk and ambiguity. *Available on Optimization Online* .
- Ghosal S, Wiesemann W (2020) The distributionally robust chance-constrained vehicle routing problem. *Operations Research* 68(3):716–732.

- Gounaris CE, Wiesemann W, Floudas CA (2013) The robust capacitated vehicle routing problem under demand uncertainty. *Operations Research* 61(3):677–693.
- Jaillet P, Qi J, Sim M (2016) Routing optimization under uncertainty. *Operations Research* 64(1):186–200.
- Kenyon AS, Morton DP (2003) Stochastic vehicle routing with random travel times. *Transportation Science* 37(1):69–82.
- Laporte G, Louveaux F, Mercure H (1992) The vehicle routing problem with stochastic travel times. *Transportation Science* 26(3):161–170.
- Lee C, Lee K, Park S (2012) Robust vehicle routing problem with deadlines and travel time/demand uncertainty. *Journal of the Operational Research Society* 63(9):1294–1306.
- Li X, Tian P, Leung SC (2010) Vehicle routing problems with time windows and stochastic travel and service times: Models and algorithm. *International Journal of Production Economics* 125(1):137–145.
- Liu S, He L, Shen ZJM (2021) On-time last-mile delivery: Order assignment with travel-time predictors. *Management Science* 67(7):4095–4119.
- Mandi J, Demirović E, Stuckey PJ, Guns T (2020) Smart predict-and-optimize for hard combinatorial optimization problems. *Proceedings of the AAAI Conference on Artificial Intelligence* 34(2):1603–1610.
- Mandl C, Minner S (2023) Data-driven optimization for commodity procurement under price uncertainty. *Manufacturing & Service Operations Management* 25(2):371–390.
- Miranda DM, Conceição SV (2016) The vehicle routing problem with hard time windows and stochastic travel and service time. *Expert Systems with Applications* 64:104–116.
- Mišić VV, Perakis G (2020) Data analytics in operations management: A review. *Manufacturing & Service Operations Management* 22(1):158–169.
- Oyola J, Arntzen H, Woodruff DL (2017) The stochastic vehicle routing problem, a literature review, Part II: solution methods. *EURO Journal on Transportation and Logistics* 6(4):349–388, ISSN 2192-4376.
- Oyola J, Arntzen H, Woodruff DL (2018) The stochastic vehicle routing problem, a literature review, part I: models. *EURO Journal on Transportation and Logistics* 7(3):193–221.
- Pessoa A, Sadykov R, Uchoa E, Vanderbeck F (2020) A generic exact solver for vehicle routing and related problems. *Mathematical Programming* 183(1):483–523.
- Rencher AC, Christensen WF (2012) *Methods of Multivariate Analysis* (John Wiley & Sons, Inc.).
- Rios I, Wets RJ, Woodruff DL (2015) Multi-period forecasting and scenario generation with limited data. *Computational Management Science* 12(2):267–295.
- Rostami B, Desaulniers G, Errico F, Lodi A (2021) Branch-price-and-cut algorithms for the vehicle routing problem with stochastic and correlated travel times. *Operations Research* 69(2):436–455.
- Sadana U, Chenreddy A, Delage E, Forel A, Frejinger E, Vidal T (2023) A survey of contextual optimization methods for decision making under uncertainty. *arXiv preprint arXiv:2306.10374* .
- Serrano B, Minner S, Schiffer M, Vidal T (2024) Bilevel optimization for feature selection in the data-driven newsvendor problem. *European Journal of Operational Research* ISSN 0377-2217.

- Shapiro A, Dentcheva D, Ruszczyński A (2014) *Lectures on Stochastic Programming: Modeling and Theory* (SIAM).
- Solomon MM (1987) Algorithms for the vehicle routing and scheduling problems with time window constraints. *Operations Research* 35(2):254–265.
- Taş D, Dellaert N, van Woensel T, De Kok T (2014a) The time-dependent vehicle routing problem with soft time windows and stochastic travel times. *Transportation Research Part C: Emerging Technologies* 48:66–83.
- Taş D, Gendreau M, Dellaert N, van Woensel T, de Kok A (2014b) Vehicle routing with soft time windows and stochastic travel times: A column generation and branch-and-price solution approach. *European Journal of Operational Research* 236(3):789–799.
- Van Parys BP, Bennouna MA (2022) Robust two-stage optimization with covariate data. *Available on Optimization Online* .
- Zhang Y, Baldacci R, Sim M, Tang J (2019) Routing optimization with time windows under uncertainty. *Mathematical Programming* 175:263–305.
- Zhang Y, Zhang Z, Lim A, Sim M (2021) Robust data-driven vehicle routing with time windows. *Operations Research* 69(2):469–485.

Appendix A. Feature Projection Function.

The FPF is a function $\mathbf{f} : \mathbb{R}^p \times \Theta \times \mathcal{V} \setminus \{0\} \mapsto \mathbb{R}^{\bar{p}}$ that generates a \bar{p} -dimensional vector of projected features given a feature vector $\mathbf{x} \in \mathbb{R}^p$, a route $\theta \in \Theta$, a node $i \in \theta$, and travel time estimates $\hat{\mathbf{t}}$. The projected features are split into groups, as follows:

Table A.4: Feature Projection Function: Predictors of the Penalty at Customer $i \in \theta$ Returned by $\mathbf{f}(\mathbf{x}, \theta, i; \hat{\mathbf{t}})$

Predictor	Group	Description
x_1, \dots, x_p	(a)	Travel time covariates (original features)
e_i	(b)	Start of time window of customer $i \in \theta$
ℓ_i	(b)	End of time window of customer $i \in \theta$
$\ell_{\rho(i)}$	(b)	End of time window of customer $\rho(i) \in \theta$ that precedes $i \in \theta$
$c_{\rho(i),i}$	(b)	Transportation cost of the arc from $\rho(i)$ to i
$\hat{\sigma}_{\rho(i),i}^2$	(b)	Estimated variance in the travel time from $\rho(i)$ to i
k_i	(b)	Position of customer i along route θ
$a_\theta(i; \underline{\mathbf{t}})$	(c)	Lower bound on arrival time at customer $i \in \theta$ with free-flow travel times $\underline{\mathbf{t}}$
$s_\theta(i; \underline{\mathbf{t}})$	(c)	Lower bound on service start time at customer $i \in \theta$ with free-flow travel times $\underline{\mathbf{t}}$
$(a_\theta(i; \underline{\mathbf{t}}) - \ell_i)^+$	(c)	Lower bound on lateness
$\pi(a_\theta(i; \underline{\mathbf{t}}) - \ell_i)$	(c)	Lower bound on penalty
$\hat{t}_{\rho(i),i}$	(d)	Predicted travel time of the arc from $\rho(i)$ to i
$a_\theta(i; \hat{\mathbf{t}})$	(d)	Arrival times at customer $i \in \theta$ given predicted travel times $\hat{\mathbf{t}}$
$s_\theta(i; \hat{\mathbf{t}})$	(d)	Service start time at customer $i \in \theta$ given predicted travel times $\hat{\mathbf{t}}$
$(a_\theta(i; \hat{\mathbf{t}}) - \ell_i)^+$	(d)	Lateness at customer $i \in \theta$ given predicted travel times $\hat{\mathbf{t}}$
$\pi(a_\theta(i; \hat{\mathbf{t}}) - \ell_i)$	(d)	Penalty at customer $i \in \theta$ given predicted travel times $\hat{\mathbf{t}}$
$\xi_\theta(i; \hat{\mathbf{t}})$	(e)	Variability model of service start time at customer $i \in \theta$ (see Appendix A.1)

Appendix A.1. Variability of service start time.

In order to derive penalty predictors that take into account travel time variability and its impact on the service start time, we introduce a measure of variability of service start time, which we denote as *service start time risk*. Given a route θ and a customer $i \in \theta$, the distribution of $\max\{e_i, a_\theta(i; \tilde{\mathbf{t}})\}$ (the service start time at customer i) is, in general, truncated, because of possible early arrivals and waiting times at customer i and at other customers previously visited. Such a truncation decreases service start time variability; therefore, a covariate for service start time risk should consider both travel time variability and the likelihood of early arrivals along a route.

Let $\Sigma = [\sigma_{ij,lm}]_{(i,j),(l,m) \in \mathcal{A}}$ be the travel times covariance, and let $\sigma_{ij}^2 = \sigma_{ij,ij}$. Given a route $\theta = (v_1, \dots, v_L)$, we denote by $\xi_\theta(i)$ the service start time risk at customer $i \in \theta$, and consider the following risk propagation model:

$$\xi_\theta(v_k) = \begin{cases} (1 - \mathcal{P}_\theta(v_k))\sigma_{0v_k}^2, & \text{if } k = 1, \\ (1 - \mathcal{P}_\theta(v_k))(\xi_\theta(v_{k-1}) + \sigma_{v_{k-1}v_k}^2 + 2\sigma_{v_{k-2}v_{k-1},v_{k-1}v_k}), & \text{otherwise,} \end{cases} \quad (\text{A.1})$$

where $\mathcal{P}_\theta(i) = \mathbb{P}(a_\theta(i; \tilde{\mathbf{t}}) < e_i \mid \mathbf{x}^{n+1})$ is the early arrival probability at customer $i \in \theta$ conditional on observed features \mathbf{x}^{n+1} , and $v_0 = 0$.

Model (A.1) propagates the variabilities of travel time and service start time along route θ as far as early arrival probabilities are low. When the early arrival probability $\mathcal{P}_\theta(i)$ is high, the service start time risk at customer i is low, since service occurs at instant e_i with high probability. In this case, the service start time risk at other customers along route θ following customer i also decreases. Note that the model accounts for travel time correlation between adjacent arcs in the network.

Service start time risk measures $\xi_\theta(i)$, $i \in \theta$, cannot be computed directly because the travel time distribution is unknown. Following our distribution-free approach, we estimate Σ and $\mathcal{P}_\theta(i)$ (and hence $\xi_\theta(i)$) from data. Let $\hat{\Sigma} = [\hat{\sigma}_{ij,lm}]_{(i,j),(l,m) \in \mathcal{A}}$ be the estimated travel times covariance (as described in Section 3.3) and let $\hat{\sigma}_{ij}^2 = \hat{\sigma}_{ij,ij}$. In the remainder of this section, we discuss how to estimate $\mathcal{P}_\theta(i)$ for

any route θ . To this end, we let $\mathbf{g} : \mathbb{R}^p \mapsto \mathbb{R}^{|\mathcal{A}|}$ be a travel time prediction model. Further, we assume that for each customer $i \in \mathcal{V} \setminus \{0\}$ a set of training routes Θ_i is available, where $i \in \theta$ for all $\theta \in \Theta_i$. This is an unrestrictive assumption as these training routes may be arbitrary routes, e.g., generated by solving other VRP models. Finally, let $\rho_\theta(v_k)$ be the node that precedes v_k in route $\theta = (v_1, \dots, v_L)$, that is, $\rho_\theta(v_k) = 0$ if $k = 1$, and $\rho_\theta(v_k) = v_{k-1}$ if $k \geq 2$.

Given a vector \mathbf{x} of travel time covariates, let $\mathbf{w}_{i,\theta}(\mathbf{x})$ be the vector of early arrival covariates, with components as described in Table A.5. Clearly, if $e_i = 0$, then we have $\mathcal{P}_\theta(i) = 0$. Further, note that if $C_\theta > e_i$, then $\mathcal{P}_\theta(i) = 0$, since we assume that $\tilde{t}_{ij} \geq c_{ij}$. Finally, if $\max_{j \in \theta \setminus \{i\}} \{e_j\} > e_i$, then we have again $\mathcal{P}_\theta(i) = 0$.

Table A.5: Components of the early arrival covariates vector $\mathbf{w}_{i,\theta}(\mathbf{x})$ at customer $i \in \theta$ given feature vector \mathbf{x}

Predictor	Description
x_1, \dots, x_p	Travel time covariates
e_i	Opening of time window
$a_\theta(i; \mathbf{g}(\mathbf{x}))$	Estimated arrival time at customer $i \in \theta$
$\hat{\sigma}_{\rho_\theta(i)i}^2$	Estimated variance in the travel time from $\rho_\theta(i)$ to i
$\max_{j \in \theta \setminus \{i\}} \{e_j\}$	Latest e_j along route θ before arriving at customer i
C_θ	Transportation cost of route θ up to customer i

Since our predicted quantity is a probability, a sensible learning model is a logistic regression. Let $S(z) = 1/(1 + \exp(-z))$ be the logistic function, and let $\mathcal{L}_{\text{null}}(a, b) = -(b \log a + (1 - b) \log(1 - a))$ be the negative log likelihood loss function. For each customer $i \in \mathcal{V} \setminus \{0\}$, we train the parameters $\hat{\phi}_i^0$ and $\hat{\phi}_i \in \mathbb{R}^{p+2}$ of the logit model:

$$\hat{\phi}_i^0, \hat{\phi}_i = \arg \min_{\phi_i^0 \in \mathbb{R}, \phi_i \in \mathbb{R}^{p+2}} \frac{1}{n|\Theta_i|} \sum_{k=1}^n \sum_{\theta \in \Theta_i} \mathcal{L}_{\text{null}} \left(S(\phi_i^0 + \phi_i^\top \mathbf{w}_{i,\theta}^k), \mathbb{I}(a_\theta(i; \mathbf{t}^k) \leq e_i) \right) + \lambda \|\phi_i\|_1,$$

where we use $\mathbf{w}_{i,\theta}^k := \mathbf{w}_{i,\theta}(\mathbf{x}^k)$, λ is the regularization parameter and $\|\phi_i\|_1$ is the ℓ_1 norm of ϕ_i .

Regularization by the ℓ_1 norm leads to sparsity in the model parameters.

Hence, for any route θ we estimate the early arrival probability at customer $i \in \theta$ by

$$\hat{\mathcal{P}}_\theta(i) = S(\hat{\phi}_i^0 + \hat{\phi}_i^\top \mathbf{w}_{i,\theta}^{n+1}).$$

Appendix B. Dynamic programming algorithm for RCSP

We present a DP algorithm for obtaining a RCSP bound. In Algorithm 1, variable $T_1[\delta, i, q]$ stores a lower bound on the reduced cost of extending a route that ends at customer i with remaining capacity q , departing from i at time δ (i.e., the arrival time at customer i is equal to δ). We relax elementarity by allowing routes with cycles but we still remove 2-cycles. Similarly, $T_2[\delta, i, q]$ stores the second best lower bound on the reduced cost. Finally, $N[\delta, i, q]$ stores the customer following i on the route associated with the best lower bound.

Algorithm 1: Dynamic programming algorithm for RCSP

Result: matrix T_1 of lower bounds on the reduced costs of route extensions

```

1  $\ell_{\max} \leftarrow \max_{i \in \mathcal{V}^+} \{\ell_i\}$  // latest end of time window among all customers
2  $\Delta t \leftarrow \ell_{\max}/40$  // define a time step
3 for  $\delta = 0, \Delta t, 2\Delta t, \dots, \ell_{\max}$  do
4    $T_1[\delta, i, q] \leftarrow \infty$ , for  $i \in \mathcal{V}^+, q = 1, \dots, Q$  // initialize matrix  $T_1$ : lower bound on reduced costs
5    $T_1[\delta, 0, q] \leftarrow 0$ , for  $q = 0, \dots, Q$  // initialize matrix  $T_1$ 
6    $T_1[\delta, i, 0] \leftarrow c_{i0}$ , for  $i \in \mathcal{V}^+$  // initialize matrix  $B$ 
7    $T_2[\delta, i, q] \leftarrow \infty$ , for  $i \in \mathcal{V}, q = 0, \dots, Q$  // initialize matrix  $T_2$ : second best cost
8    $N[\delta, i, q] \leftarrow 0$ , for  $i \in \mathcal{V}, q = 0, \dots, Q$  // initialize matrix  $N$ : next customer in the route
9   for  $q = 1, \dots, Q$  do
10    for  $i \in \mathcal{V}^+$  do
11       $T_1[\delta, i, q] \leftarrow T_1[\delta, i, q - 1]$ 
12       $T_2[\delta, i, q] \leftarrow T_2[\delta, i, q - 1]$ 
13       $N[\delta, i, q] \leftarrow N[\delta, i, q - 1]$ 
14      for  $j \in \mathcal{V}^+$  do
15        if  $j = i$  or  $q_j > q$  or arc  $(i, j)$  is forbidden by branching then
16          continue // does not extend label  $L$  to customer  $j$ 
17        if  $N[\delta, j, q - q_j] \neq i$  then
18           $v \leftarrow c_{ij} - \gamma_j + T_1[\delta, j, q - q_j] + \pi(\delta - \ell_j)$  // xxx
19        else
20           $v \leftarrow c_{ij} - \gamma_j + T_2[\delta, j, q - q_j] + \pi(\delta - \ell_j)$  // avoid 2-cycles
21        if  $v < T_1[i, q]$  then
22           $T_2[\delta, i, q] \leftarrow T_1[\delta, i, q]$  // move best to second best
23           $T_1[\delta, i, q] \leftarrow v$  // set new best
24           $N[\delta, i, q] \leftarrow j$  // set next customer
25        else if  $v < T_2[\delta, i, q]$  then
26           $T_2[\delta, i, q] \leftarrow v$  // just update second best
27 return  $T_1$ 

```

Appendix C. Proof of completion bounds

We provide proofs for the RCSP and knapsack bounds in the following.

Proof of Proposition 1. From the definition of the RCSP bound in Equation (21), we have:

$$\begin{aligned}
0 &\stackrel{(a)}{\leq} \bar{C}_\theta + \widehat{T}_{\text{RCSP}}(i, Q - q_\theta) \\
&\stackrel{(b)}{\leq} \bar{C}_\theta - c_{i0} + c_{iu_1} + \pi(\delta_{\theta \oplus u_1} - \ell_{u_1}) - \gamma_{u_1} + c_{u_1 0} + \widehat{T}_{\text{RCSP}}(u_1, Q - q_{\theta \oplus u_1}) \\
&\stackrel{(c)}{\leq} \bar{C}_\theta - c_{i0} + c_{iu_1} + \pi(\delta_{\theta \oplus u_1} - \ell_{u_1}) - \gamma_{u_1} + c_{u_1 0} \\
&\quad - c_{u_1 0} + c_{u_1 u_2} + \pi(\delta_{\theta \oplus u_1 \oplus u_2} - \ell_{u_2}) - \gamma_{u_2} + c_{u_2 0} \\
&\quad \dots \\
&\quad - c_{u_{L-1} 0} + c_{u_{L-1} u_L} + \pi(\delta_{\theta \oplus \varepsilon} - \ell_{u_L}) - \gamma_{u_L} + c_{u_L 0} + \widehat{T}_{\text{RCSP}}(u_L, Q - q_{\theta \oplus \varepsilon}) \\
&\stackrel{(d)}{=} \bar{C}_\theta - c_{i0} + c_{iu_1} + \sum_{j=2}^L c_{u_{j-1} u_j} + c_{u_L 0} + \sum_{j=1}^L \left(\pi(\delta_{\theta \oplus u_1 \oplus \dots \oplus u_j} - \ell_{u_j}) - \gamma_{u_j} \right) + \widehat{T}_{\text{RCSP}}(u_L, Q - q_{\theta'}) \\
&\stackrel{(e)}{\leq} \bar{C}_\theta - c_{i0} + c_{iu_1} + \sum_{j=2}^L c_{u_{j-1} u_j} + c_{u_L 0} + \sum_{j=1}^L \left(\sum_{\omega \in \Omega} \alpha^\omega \cdot \pi(a_{\theta'}(u_j; \mathbf{t}^\omega) - \ell_{u_j}) - \gamma_{u_j} \right) + \widehat{T}_{\text{RCSP}}(u_L, Q - q_{\theta'}) \\
&\stackrel{(f)}{=} \bar{C}_{\theta'} + \widehat{T}_{\text{RCSP}}(u_L, Q - q_{\theta'}) \stackrel{(g)}{\leq} \bar{C}_{\theta'}.
\end{aligned}$$

Inequality (b) follows from the fact that extending path θ to customer u_1 cannot lead to a smaller bound than the bound associated with the optimal path extension from the minimization operator in Equation (21). In Inequality (c), the same argument holds when extending path $\theta \oplus u_1$ to customers u_2, \dots, u_j . In Equation (d) we rearrange the terms, and Inequality (e) is due to the fact that, given a path θ ending at customer j :

$$\delta_\theta \leq \tau_\theta \leq a_\theta(j; \mathbf{t}^\omega), \quad \forall \omega \in \Omega \quad (\text{C.1})$$

Finally, Equality (f) is due to the resource extension function for the reduced cost given by Equation (18), and Inequality (g) holds since going from u_L back to the depot incurs no additional cost and can not improve the completion bound. \square

Proof of Proposition 2. From the resource extension function given by Equation (18), we have:

$$\begin{aligned}
\bar{C}_{\theta'} &\stackrel{(a)}{=} \bar{C}_\theta - c_{i0} + c_{iu_1} + \sum_{j=2}^L c_{u_{j-1}u_j} + c_{u_L0} + \sum_{j=1}^L \left(\sum_{\omega \in \Omega} \alpha^\omega \cdot \pi(a_{\theta'}(u_j; \mathbf{t}^\omega) - \ell_{u_j}) - \gamma_{u_j} \right) \\
&\stackrel{(b)}{\geq} \bar{C}_\theta + \sum_{j=1}^L \left(\sum_{\omega \in \Omega} \alpha^\omega \cdot \pi(a_{\theta'}(u_j; \mathbf{t}^\omega) - \ell_{u_j}) - \gamma_{u_j} \right) \\
&\stackrel{(c)}{\geq} \bar{C}_\theta + \sum_{j=1}^L \left(\pi(\tau_\theta + \min_{\omega \in \Omega} t_{iu_j}^\omega - \ell_{u_j}) - \gamma_{u_j} \right) \\
&\stackrel{(d)}{=} \bar{C}_\theta + \sum_{l \in \mathcal{V} \setminus \{0\}} -v_{il}(\theta) z_l^* \stackrel{(e)}{\geq} \bar{C}_\theta + \hat{T}_{ks}(i, Q - q_\theta) \geq 0
\end{aligned}$$

where Inequality (b) is due to the triangle inequality, which implies that the cost of a route cannot decrease if we add customers to it. Inequality (c) is a consequence of Equation (23) and the fact that adding more customers to a route between i and u_j can only increase the arrival time at customer u_j . Equality (d) holds by our definition of the knapsack values. Inequality (e) is due to the optimality of the knapsack solution and the definition of the completion bound. \square

Appendix D. Detailed results for instances with 25 customers

The BP&C method could find optimal solutions for all instances with 25 customers within the predetermined time limit. In the following, we analyze the test cost results under the different generative models of travel times.

Linear generative model. Table D.6 reports the test costs of different data-driven approaches for instances with 25 customers and a linear generative model. Among the practical models, we highlight with boldface numbers the models that achieve the lowest cost on each instance. For PTO-F and “Full” models, we highlight the results in boldface whenever one of the practical models achieves equal or lower test cost. CSAA achieves the lowest test costs among the practical models for most instances. For C-type instances, most models achieve the full information lower bound.

Exponential generative model. Table D.7 reports the test costs for instances with 25 customers and an exponential generative model. We observe higher deviations from the lower bound in this setting

than in the previous results under the linear generative model. On average, CSAA is superior to the other models. We also note that P-NN is superior on a number of instances. However, the lower bound is achieved only in a single instance, illustrating the greater difficulty of solving the contextual stochastic VRPTW under a nonlinear generative model.

Sigmoidal generative model. Table D.8 reports test costs for instances with 25 customers and a sigmoidal generative model. As before, on average, CSAA is superior to the other models. For some instances, CSAA is outperformed by SAA. In this setting, SAA is superior to PTO and P-NN, in contrast to the results with linear and exponential generative models.

Comparison of generative models. Table D.9 compares the average test costs of all considered approaches under the different generative models of travel times. Considering the practical models, CSAA achieves the lowest test costs on average. PTO-F is superior to CSAA for the exponential and sigmoidal instances, indicating that the PTO framework could be the best approach in those settings, provided that one can train a model that can predict the conditional expected travel times perfectly. Further investigation is needed to assess how well the PTO framework can perform in practice under different predictive models. However, in all settings, the average test cost performance of CSAA is close to that of PTO-F, meaning that CSAA would be on par with PTO-F even in the unlikely case in which one could predict the true conditional expected travel times.

Table D.6: Test cost results for instances with linear generative model and 25 customers

Instance	D-avg	SAA	PTO-OLS	PTO-kNN	SAA-kNN	CSAA	RSAA	P-NN	PTO-F	Full (Abs.)
R101	2.88	1.48	1.03	1.63	1.06	0.09	0.05	1.68	1.03	649.6
R102	2.13	2.46	0.02	1.27	1.04	0.02	0.02	0.56	0.02	576.5
R103	8.62	0.17	2.69	2.77	0.00	0.06	0.09	0.09	0.00	465.4
R104	13.98	2.94	1.29	5.76	0.34	0.00	0.00	0.02	0.8	435.6
R105	10.5	3.4	0.28	8.13	2.51	0.06	0.06	0.07	0.28	544.9
R106	75.0	0.00	1.89	42.85	8.32	0.00	0.84	2.67	5.85	502.4
R107	0.16	0.16	0.25	0.25	0.91	0.00	0.00	0.3	0.25	437.6
R108	5.34	6.12	0.9	3.37	0.9	0.17	0.05	0.34	0.85	411.9
R109	1.34	1.98	0.02	0.75	0.77	0.02	0.02	0.02	0.02	455.0
R110	22.39	4.51	0.63	4.03	2.2	0.04	0.04	0.17	0.41	458.7
R111	108.97	12.23	0.89	31.46	27.09	0.13	0.13	1.02	1.44	450.4
R112	29.73	5.17	1.73	29.73	5.87	0.12	0.02	0.1	0.9	410.3
C101	0.00	0.00	0.00	0.00	3.1	0.00	0.00	0.00	0.00	196.5
C102	0.00	0.00	0.00	0.00	0.77	0.00	0.00	0.92	0.00	195.8
C103	-	-	-	-	-	-	-	-	-	-
C104	0.00	0.00	0.00	0.00	0.00	0.00	0.00	0.21	0.00	187.5
C105	0.00	0.00	0.00	0.00	0.00	0.00	0.00	0.00	0.00	191.8
C106	0.00	0.00	0.00	0.00	0.00	0.00	0.00	0.00	0.00	194.3
C107	0.00	0.00	0.00	0.00	0.00	0.00	0.00	0.00	0.00	191.8
C108	0.00	0.00	0.00	0.00	0.00	0.00	0.00	0.00	0.00	191.8
C109	0.00	0.00	0.00	0.00	0.00	0.00	0.00	0.00	0.00	191.8
RC101	30.89	1.73	5.96	45.5	12.68	0.02	0.04	4.03	5.7	533.2
RC102	56.1	17.4	1.43	42.96	2.68	0.08	0.03	0.54	1.94	392.5
RC103	15.55	15.17	2.67	12.67	0.12	0.03	0.03	1.74	2.82	344.0
RC104	2.88	0.94	2.88	5.73	1.72	0.38	0.44	2.66	0.63	319.3
RC105	2.67	1.24	1.38	1.15	0.48	0.55	0.55	1.34	0.6	419.1
RC106	16.89	7.54	5.41	10.76	6.31	1.86	1.65	6.79	2.48	375.4
RC107	10.93	1.3	3.97	9.33	0.91	0.29	0.16	3.09	2.63	307.5
RC108	2.68	2.68	0.07	3.74	0.26	0.13	0.13	0.33	0.07	302.3
Average	14.99	3.16	1.26	9.42	2.86	0.14	0.16	1.02	1.03	369.03

Table D.7: Test cost results for instances with exponential generative model and 25 customers

Instance	D-avg	SAA	PTO-OLS	PTO-kNN	SAA-kNN	CSAA	RSAA	P-NN	PTO-F	Full (Abs.)
R101	8.3	4.08	0.33	3.29	2.49	0.7	0.52	0.33	0.24	1259.2
R102	8.21	11.71	2.74	5.81	5.13	1.22	1.33	1.99	0.92	779.6
R103	34.77	8.01	4.05	15.32	6.94	1.32	1.03	2.93	1.7	522.9
R104	14.99	3.11	7.26	13.58	8.48	3.74	2.76	4.5	3.01	510.9
R105	51.75	25.06	4.98	10.67	9.76	4.11	4.15	10.64	1.99	804.5
R106	7.61	8.06	1.3	2.56	2.27	1.91	1.19	0.54	1.08	538.6
R107	356.78	46.89	3.43	20.96	6.54	0.86	0.34	0.6	3.51	498.2
R108	34.38	10.64	3.67	12.74	4.2	0.49	0.79	1.2	3.67	466.3
R109	103.98	21.15	5.13	14.67	2.87	2.73	3.75	2.78	2.46	557.5
R110	25.27	4.3	4.32	5.36	1.96	1.57	1.98	1.63	2.14	509.4
R111	31.54	23.4	1.43	30.21	12.38	1.26	0.99	1.35	1.65	586.2
R112	103.67	14.45	5.89	53.55	13.41	6.93	6.0	1.93	3.83	460.1
C101	176.85	8.42	47.02	178.59	39.88	4.33	5.6	1.66	9.31	258.8
C102	33.29	6.4	5.75	20.71	4.32	1.21	0.86	2.51	8.26	231.3
C103	20.52	0.35	12.53	11.43	4.49	1.95	0.9	1.75	6.54	200.3
C104	-	-	-	-	-	-	-	-	-	-
C105	104.16	13.72	26.16	104.16	13.16	13.34	17.5	8.32	35.03	233.2
C106	19.29	2.05	9.0	22.45	5.39	0.84	2.05	2.16	3.49	263.3
C107	0.78	0.78	0.78	0.78	0.78	0.78	0.78	0.78	0.78	192.8
C108	0.10	0.10	0.10	0.10	0.10	0.10	0.10	0.10	0.10	192.7
C109	0.00	0.00	0.00	0.00	0.00	0.00	0.00	0.00	0.00	191.8
RC101	91.45	78.9	20.86	25.11	26.11	22.34	20.85	20.93	2.67	674.5
RC102	126.85	39.67	16.3	119.7	4.66	4.32	4.45	2.88	2.02	573.5
RC103	42.63	6.33	9.85	14.79	4.94	5.81	5.81	11.14	5.37	497.5
RC104	53.44	19.32	4.91	7.56	14.94	5.92	5.87	5.75	6.95	415.6
RC105	15.94	5.85	4.62	15.31	4.5	2.44	2.71	4.84	5.76	553.8
RC106	350.2	21.77	10.36	27.22	6.61	2.07	5.06	7.42	5.55	537.4
RC107	11.18	5.46	26.13	11.67	5.87	10.59	22.0	21.92	10.63	470.4
RC108	106.85	20.28	12.87	53.0	16.62	8.54	9.9	9.29	9.27	397.0
Average	69.1	14.65	8.99	28.62	8.17	3.98	4.62	4.71	4.93	477.76

Table D.8: Test cost results for instances with sigmoidal generative model and 25 customers

Instance	D-avg	SAA	PTO-OLS	PTO- k NN	SAA- k NN	CSAA	RSAA	P-NN	PTO-F	Full (Abs.)
R101	14.06	11.3	13.04	15.14	10.2	6.31	7.34	11.27	8.57	1100.6
R102	123.88	30.19	25.34	79.38	39.03	21.92	14.00	16.09	9.44	926.2
R103	111.72	19.45	26.71	65.46	12.78	10.55	9.26	19.47	13.97	529.0
R104	102.4	16.32	38.33	61.99	27.79	17.44	14.36	27.87	21.28	500.1
R105	163.67	27.7	35.37	37.17	21.83	26.02	18.68	25.07	12.17	702.8
R106	55.21	12.21	56.77	49.9	12.03	10.34	11.69	25.38	14.79	572.5
R107	106.36	13.47	91.1	76.81	16.12	15.57	13.74	36.45	28.34	514.4
R108	118.65	8.65	40.72	86.72	13.81	17.15	11.27	24.16	15.58	473.0
R109	81.88	53.94	54.22	106.62	30.46	11.85	15.78	31.13	21.04	567.9
R110	180.97	12.7	20.84	42.72	11.09	8.16	10.46	13.74	18.81	508.7
R111	24.16	11.01	20.08	20.39	14.9	7.82	8.13	16.33	14.68	495.9
R112	88.22	12.28	46.23	63.7	17.31	11.27	19.93	29.36	24.87	455.1
C101	189.53	12.97	137.29	67.08	14.62	21.97	18.33	39.35	127.22	272.2
C102	35.91	17.81	53.93	44.82	19.52	17.81	19.77	32.02	69.02	239.2
C103	79.54	10.61	53.04	63.37	15.79	2.62	7.42	8.56	29.73	210.2
C104	-	-	-	-	-	-	-	-	-	-
C105	191.87	14.78	181.6	186.98	136.84	132.73	134.21	145.46	154.58	243.5
C106	10.33	8.43	49.47	38.37	7.88	16.09	23.27	33.13	91.13	272.9
C107	101.25	101.2	43.13	101.25	101.34	59.64	59.64	43.13	101.25	216.3
C108	45.79	45.79	45.79	45.79	39.76	45.79	45.79	45.79	45.79	204.2
C109	31.37	31.37	31.37	31.37	31.37	31.37	31.37	31.37	31.37	191.9
RC101	52.94	46.07	60.23	61.72	35.21	37.71	35.0	31.80	7.6	783.1
RC102	90.07	19.06	105.58	92.49	24.62	51.48	39.6	44.91	64.77	558.9
RC103	175.45	25.33	64.98	87.81	33.82	33.37	39.18	53.55	36.04	448.9
RC104	223.16	49.96	70.28	96.86	36.56	29.07	39.9	60.37	62.82	404.5
RC105	285.53	21.61	86.97	162.95	31.7	25.52	40.26	46.15	47.67	571.6
RC106	320.05	27.7	83.45	66.89	17.76	15.04	24.95	36.59	64.34	471.4
RC107	432.47	29.59	111.35	245.93	40.74	37.07	29.59	61.34	47.04	485.3
RC108	285.87	29.62	129.35	149.61	54.36	32.88	55.46	84.66	68.14	410.6
Average	132.94	25.75	63.45	80.33	31.04	26.95	28.51	38.38	44.72	476.1

Table D.9: Average test costs and percentage gaps to the full-knowledge model for instances with 25 customers

	Generative model	D-avg	SAA	PTO-OLS	PTO- k NN	SAA- k NN	CSAA	RSAA	P-NN	PTO-F	Full
\hat{R}	Linear	436.0	382.1	374.4	411.0	381.8	369.6	369.7	373.3	373.6	369.0
	Exponential	809.5	559.0	515.5	596.6	515.8	497.3	499.8	502.0	496.5	477.8
	Sigmoidal	1102.7	593.2	751.4	844.7	607.1	588.9	592.7	638.9	642.0	476.1
Gap(%)	Linear	18.16	3.55	1.46	11.38	3.47	0.16	0.17	1.17	1.25	0.00
	Exponential	69.42	16.99	7.89	24.86	7.95	4.08	4.61	5.06	3.91	0.00
	Sigmoidal	131.61	24.60	57.82	77.42	27.52	23.69	24.49	34.19	34.85	0.00

Appendix E. Detailed results for instances with 50 customers

With 50 customers, we could not solve all instances to optimality. To conduct a fair comparison between the models, we consider in the following analyses only instances for which all models could

find optimal solutions or integer feasible solutions with an optimality gap of at most 0.01.

Linear generative model. Table E.10 shows test cost results for 22 instances that could be solved to an optimality gap of at most 1%. Among the practical models, CSAA achieves the lowest test costs in all instances. The full-information lower bound is achieved in 5 out of the 22 instances. Notably, the test costs of CSAA are smaller than or equal to those of PTO-F in all instances.

Exponential generative model. Table E.11 reports the test costs of different data-driven approaches for 24 instances that could be solved to an optimality gap of at most 1%. For most instances, CSAA has the lowest test costs among the practical models. Moreover, CSAA is also superior to PTO-F, on average.

Sigmoidal generative model. Table E.12 reports the test cost of different data-driven approaches for 21 that could be solved to an optimality gap of at most 1%. As before, on average, CSAA is superior to the other practical models. However, we observe a larger gap to the full-information lower bound.

Comparison of generative models. We compare the average test costs achieved by the different methods across the different generative models in Table E.13. For linear and exponential travel times, CSAA has the lowest average test costs. For sigmoidal travel times, we observe significantly larger gaps. In this setting, CSAA has a full-information gap of 32.93%, close to PTO-F, with 32.20%.

Table E.10: Test cost results for instances with linear generative model and 50 customers

Instance	D-avg	SAA	PTO-OLS	PTO- k NN	SAA- k NN	CSAA	RSAA	PTO-F	Full
R101	25.36	5.84	1.11	10.97	3.48	0.7	0.66	0.97	1237.0
R102	18.32	3.72	0.99	16.39	1.44	0.16	0.21	1.01	1155.8
R103	6.96	2.91	3.05	4.53	1.99	0.27	0.42	1.29	850.2
R104	-	-	-	-	-	-	-	-	-
R105	51.25	6.4	2.44	23.05	5.86	0.67	0.28	1.28	994.4
R106	-	-	-	-	-	-	-	-	-
R107	7.52	2.12	1.81	16.82	2.63	0.3	0.18	2.12	772.8
R108	-	-	-	-	-	-	-	-	-
R109	7.64	3.98	4.16	7.75	0.52	0.23	0.24	1.81	828.7
R110	35.0	3.22	1.45	14.33	5.92	0.44	0.22	0.99	758.5
R111	32.81	3.6	2.26	19.8	6.85	0.12	0.08	1.58	738.5
R112	-	-	-	-	-	-	-	-	-
C101	1.66	21.32	1.66	1.66	3.09	0.00	0.00	1.66	379.0
C102	4.7	4.7	0.05	4.7	1.55	0.05	0.05	0.05	367.8
C103	-	-	-	-	-	-	-	-	-
C104	-	-	-	-	-	-	-	-	-
C105	0.00	0.00	0.00	0.00	0.00	0.00	0.00	0.00	363.2
C106	1.52	9.57	1.52	1.52	1.52	0.95	0.95	1.52	387.5
C107	0.00	0.00	0.00	0.00	0.00	0.00	0.00	0.00	363.2
C108	0.00	0.00	0.00	0.00	0.00	0.00	0.00	0.00	363.2
C109	0.00	0.00	0.00	0.00	0.00	0.00	0.00	0.00	363.2
RC101	54.67	6.1	5.9	16.93	6.23	1.28	1.09	4.91	1130.4
RC102	93.37	9.48	3.92	24.37	6.37	0.75	0.81	2.4	987.5
RC103	45.81	5.42	4.35	22.79	11.45	0.10	0.46	2.13	774.5
RC104	-	-	-	-	-	-	-	-	-
RC105	47.79	2.21	7.64	40.57	17.12	0.6	0.44	4.59	917.1
RC106	27.19	5.22	4.55	17.09	3.17	0.91	0.65	4.77	879.3
RC107	56.66	5.72	1.82	18.36	2.18	0.26	0.09	2.71	692.7
RC108	-	-	-	-	-	-	-	-	-
Average	24.68	4.83	2.32	12.46	3.87	0.37	0.33	1.7	728.79

Table E.11: Test cost results for instances with exponential generative model and 50 customers

Instance	D-avg	SAA	PTO-OLS	PTO-kNN	SAA-kNN	CSAA	RSAA	PTO-F	Full
R101	10.48	10.82	3.14	9.02	4.51	1.75	2.29	1.63	1466.0
R102	45.24	15.37	3.4	8.94	6.75	2.81	2.66	1.28	1821.7
R103	20.0	18.88	5.54	11.45	9.37	3.93	3.92	3.05	1679.8
R104	31.36	8.07	21.56	18.97	3.59	8.09	13.81	6.43	794.4
R105	4.76	4.33	7.89	3.59	3.01	4.72	5.33	3.36	1252.7
R106	-	-	-	-	-	-	-	-	-
R107	198.4	23.5	13.08	34.34	11.52	4.12	4.6	5.21	907.8
R108	-	-	-	-	-	-	-	-	-
R109	24.21	11.09	6.54	7.95	5.43	2.44	3.23	5.33	975.9
R110	-	-	-	-	-	-	-	-	-
R111	158.52	16.74	4.38	21.72	4.78	3.78	3.92	6.69	887.8
R112	14.73	7.8	5.37	24.43	6.52	3.45	3.23	6.15	756.5
C101	4.79	1.85	6.97	4.9	2.48	1.65	1.69	7.05	492.3
C102	5.7	0.13	2.74	2.74	0.99	0.65	1.12	2.41	473.7
C103	-	-	-	-	-	-	-	-	-
C104	-	-	-	-	-	-	-	-	-
C105	124.2	6.62	12.26	70.73	5.23	3.79	4.06	12.74	438.0
C106	66.09	7.29	7.97	26.75	6.51	9.75	5.75	7.49	500.5
C107	113.86	60.36	3.89	113.86	7.64	2.64	2.64	3.89	393.8
C108	0.14	0.14	0.63	0.14	0.14	0.14	0.22	0.69	364.0
C109	0.00	0.00	0.00	0.00	0.00	0.00	0.00	0.00	363.2
RC101	120.37	44.11	5.5	18.79	64.71	3.37	4.64	2.06	1663.0
RC102	96.18	49.45	14.25	24.92	25.28	7.31	9.02	3.93	1605.4
RC103	44.07	15.06	7.25	18.17	6.69	2.51	4.28	5.2	1029.9
RC104	-	-	-	-	-	-	-	-	-
RC105	39.43	17.38	19.16	14.49	8.52	4.09	10.17	5.56	1235.6
RC106	109.79	55.04	13.84	46.25	35.6	9.23	13.02	4.87	1181.6
RC107	58.82	6.72	98.41	32.39	7.36	12.33	20.5	9.71	928.5
RC108	-	-	-	-	-	-	-	-	-
Average	58.69	17.31	11.99	23.39	10.3	4.21	5.46	4.76	964.19

Table E.12: Test cost results for instances with sigmoidal generative model and 50 customers

Instance	D-avg	SAA	PTO-OLS	PTO- k NN	SAA- k NN	CSAA	RSAA	PTO-F	Full
R101	87.09	31.48	43.26	54.85	27.75	21.85	29.31	8.52	2179.0
R102	131.73	53.93	53.77	69.1	53.27	29.65	30.23	18.79	1732.0
R103	241.33	46.09	76.05	90.64	26.26	26.61	35.35	17.02	1627.7
R104	-	-	-	-	-	-	-	-	-
R105	303.68	23.6	32.32	104.4	16.23	16.23	17.99	25.09	1278.4
R106	252.94	43.82	106.23	107.35	42.77	28.46	22.93	50.4	1021.1
R107	233.67	32.1	92.73	81.15	31.91	23.07	25.51	37.18	940.9
R108	-	-	-	-	-	-	-	-	-
R109	261.41	16.81	72.51	156.4	26.91	19.46	22.79	41.33	978.7
R110	167.15	18.02	80.05	107.21	35.25	26.35	23.18	44.34	862.7
R111	164.21	26.28	80.91	115.21	31.36	23.87	30.57	44.54	873.8
R112	170.69	28.15	83.54	144.91	37.41	29.05	15.94	33.91	795.3
C101	186.14	16.02	59.32	62.29	25.45	49.13	29.6	63.04	532.5
C102	128.54	16.09	108.06	124.41	24.31	21.4	24.45	48.58	506.0
C103	-	-	-	-	-	-	-	-	-
C104	-	-	-	-	-	-	-	-	-
C105	-	-	-	-	-	-	-	-	-
C106	-	-	-	-	-	-	-	-	-
C107	52.86	52.86	52.68	52.86	52.46	52.26	52.68	52.86	402.4
C108	-	-	-	-	-	-	-	-	-
C109	12.25	12.25	12.25	12.00	12.8	12.00	12.25	12.74	364.1
RC101	228.78	33.32	89.05	80.05	36.36	46.11	53.35	9.24	2619.1
RC102	292.43	97.24	88.67	168.9	79.34	57.24	68.13	41.78	1337.6
RC103	509.92	80.08	143.89	143.32	77.7	32.20	37.6	47.19	1021.2
RC104	-	-	-	-	-	-	-	-	-
RC105	262.02	36.06	84.24	294.37	76.76	50.57	51.29	27.66	1422.8
RC106	203.06	44.88	90.33	90.65	35.20	41.64	39.01	72.9	1100.6
RC107	477.15	21.88	149.12	237.37	36.3	34.21	26.74	54.2	982.0
RC108	-	-	-	-	-	-	-	-	-
Average	218.35	36.55	79.95	114.87	39.29	32.07	32.44	37.57	1128.9

Table E.13: Average test costs and percentage gaps to the full-knowledge model for instances with 50 customers

	Gen. model	D-avg	SAA	PTO-OLS	PTO- k NN	SAA- k NN	CSAA	RSAA	PTO-F	Full
\hat{R}	Linear	953.4	764.5	749.1	839.7	762.1	732.1	731.7	743.5	728.8
	Exponential	1549.8	1160.9	1082.4	1159.9	1096.5	1007.3	1021.7	1006.1	964.2
	Sigmoidal	3690.0	1570.5	2029.8	2440.4	1588.8	1500.7	1524.4	1492.4	1128.9
Gap(%)	Linear	30.83	4.90	2.78	15.22	4.57	0.46	0.40	2.02	0.00
	Exponential	60.73	20.40	12.26	20.30	13.72	4.47	5.96	4.34	0.00
	Sigmoidal	226.87	39.12	79.80	116.18	40.73	32.93	35.04	32.20	0.00